On Microphase Separation of Block Copolymers in an Electric Field: Four Universal Classes

Eugene Gurovich*

Groupe De Physico-Chimie Theorique, ESPCI, 75231 Paris Cedex 05, France

Received January 13, 1994; Revised Manuscript Received August 16, 1994®

ABSTRACT: A microscopic statistical theory of homopolymer and copolymer melts in an electric field is developed. The nonlinear dielectric properties of a homopolymer melt in an electric field are described, the dipole–dipole interaction between the monomers being taken self-consistently into account. For diblocks, the order–disorder transition is studied in the framework of the random phase approximation. We predict that copolymer melts reveal four different universal types of behavior under external fields: $\mathcal{A}$, $\mathcal{B}$, $\mathcal{C}$, and $\mathcal{D}$. To determine what class a copolymer melt belongs to, the only relevant parameters turn out to be: f, the fraction of monomers A in a chain, and parameters $S^{(A)}$ and $S^{(B)}$, which characterize how many times the radii of gyration of blocks A and B increase, respectively, along an applied electric field. Class $\mathcal{A}$ represents strongly degenerated-in-electric-field copolymers, for which the anisotropic parts of the monomer A and B polarizabilities are equal. Near the spinodal point, X-ray scattering should reveal that critical wave vectors form an ellipsoid. After microphase separation, mesophases with nonfixed periodicity (which depends upon the direction of the symmetry breaking with respect to an electric field) appear. With increasing χN, these mesophases are three-dimensional triclinic, two-dimensional monoclinic, and one-dimensional lamellar structures. If the pattern appears spontaneously oriented along the electric field, the first two structures are body-centered tetragonal and honeycomb (hexagonal) structures, respectively. The spinodal line and lines of first-order transitions between mesophases are predicted to not depend on the electric field and coincide with those for zero electric field. For class $\mathcal{B}$, X-ray scattering should reveal that critical fluctuations are concentrated in Q-space on two rings, which are perpendicular to the electric field. The temperature of the transition does not depend on the electric field but is different from that for zero electric field (only if $f \neq 0.5$). For a given composition f and an applyed field, the angle between the field and the normal to the lamellar layers is fixed (does not depend on χN). For any composition f, a second-order transition occurs from a disordered melt to a lamellar phase without intermediate structures. For class $\mathcal{C}$, only fluctuations oriented strictly along the electric field diverge at the spinodal point. For any composition f, a lamellar phase oriented perpendicularly to the electric field appears by a second-order transition from a homogeneous melt. The transition temperature and the pattern periodicity do depend on the electric field. For class $\mathcal{D}$, in Q-space, critical wave vectors form a ring perpendicularly to the electric field. For any composition f with increasing χN, a two-dimensional honeycomb and a lamellar structure oriented strictly parallel to the electric field appear by first-order transitions. The transition temperatures and the pattern periodicity depend on the applied field. In symmetric copolymers, reentrant disorder → order → disorder microphase transitions and orientational and reorientational phase transitions should be observed with an increase of the electric field intensity. Experimentally observable consequences, crucial for verification of the theory, and possible applications are discussed.

1. Introduction

It is well-known that in block copolymers the incompatibility of units' sequences results in various distinct structures upon lowering the temperature and (or) increasing the degree of polymerization. The past few years have seen a renewal of interest[1] in microphase separation in copolymer melts under external forces. The application of flow[2] and electric field[3] have been shown to cause alignment of microstructures and shift transition temperatures.

The effect of an electric field on diblock copolymers patterns and on the order–disorder transition temperature was recently discussed[3] by Amundson *et al.* Two very important phenomena were observed experimentally in poly(styrene-*block*-methyl methacrylate) melt. Firstly it was noticed that the lamellar structure can be aligned by cooling through the microphase separation transition in an electric field. Secondly it was observed that the ordered phase persists above the order–disorder transition (where it would not be thermodynamically stable in the absence of an electric field). The experimental SAXS results were supported by a theoretical model.[3] The alignment process was understood in terms of nucleation and reorientation of ordered domains: once they grow to sufficient size they are reoriented by the electric field. The reorientation of the domains occurs due to the composition-pattern-dependent electrostatic contributions, which implies that in an electric field certain orientations are thermodynamically favored over others (see formulas 1 and 2 in ref 3). A shift in the order–disorder transition follows as a consequence of its first-order character: the persistence of microscopic alignment even after heating the material 14 °C above the order–disorder temperature (defined for zero-electric field) was treated as a superheated state.

The present work is concerned with a very different approach, namely, the mean-field theory. All the fluctuations are negligible and no growth of the domain structure, through nucleations and reorientation, occurs. The ordered phase appears by a weak first-order transition over all the volume of the melt. All the states are considered to be in the full thermodynamical equilibria and superheated metastable phases will not be discussed. In such a picture, the argumentation of Amundson *et al.* cannot be used and another approach is needed.

* *Present address:* Department of Physics, The Institute of Theoretical Physics, Technion, 32000, Haifa, Israel.

® Abstract published in *Advance ACS Abstracts,* November 1, 1994.

0024-9297/94/2227-7339$04.50/0 © 1994 American Chemical Society

We concentrate on the behavior of block copolymers in the presence of the electric field near the spinodal point. A microscopic statistical theory based on the random phase approximation will be developed. Particularly, we will show that in an applied electric field a symmetrical poly(styrene-*block*-methyl methacrylate) melt seems to belong to the so-called universal class B: the order–disorder transition temperature is different from that observed for zero electric field and the lamellar phase appears from the disordered phase already aligned by an applied electric field.

Let us give a qualitative description of the influence of an electric field on the microphase separation to indicate, first of all, the guidelines along which our theory is constructed. We will consider molten diblock nonpolar copolymers, which have no appreciable molecular or segmental dipole moments. [For instance, such blocks could be made from segments $(CH_2)_n$, $(CH_2C(CH_3)_2)_n$, or $(CF_2)_n$]. All the chains have the same degree of polymerization, N, and the same composition, f. The polydispersity of the chains will be neglected. Blocks will be assumed to have the same statistical segment length and the same volume per repeat unit. Our analysis will be limited to the situations where full thermal equilibrium is achieved. Polarizability tensors of A and B units are assumed to have uniaxial symmetry, the main axes being directed along and perpendicular to the bonds $\vec{a}$.

An understanding of the microphase separation transition in molten copolymers under an electric field requires not only a study of microdomain structures but also a study of the homogeneous disordered phase. We start in section 2 from an ideal chain in an electric field. The application of an electric field gives rise to chain birefringence:[6,7] its statistical properties differ from those of an ideal Gaussian chain. The square of the radii of gyration along an applied field is shown to be S times larger than that in a zero field. The parameter S depends upon the applied electric field.

As for real melts, the picture is oversimplified, since the long-range dipole–dipole interaction between polarized units is not taken into account. However, in spite of the long-range dipole–dipole interaction, in a homopolymer melt the chains conserve their "birefringed" conformation. Indeed, the inversion of any Kth bond vector $\vec{a}_K \rightarrow -\vec{a}_K$ (when all others bonds are fixed) does not change the chain free energy after reversing the dipole moment ($\vec{P}_K \rightarrow -\vec{P}_K$) of that bond. So, the inversion of the bond direction does not change the statistical weight of the chain conformation. As a result, a random walk process with different probabilities to go along and perpendicular to the electric field describes conformations of a homopolymer chain in a melt.

In section 3 the self-consistent approximation to take quantitatively into account the dipole–dipole interactions is developed. The chain conformation is described by the same parameter S, which is a function not of the applied but rather of the internal electric field. Both electric fields, the experimentally applied and the internal one, are related (in the electrostatic theory of continuous medium[8]) by a nonlinear integral equation. This latter equation was written for several common experimental geometries. In section 4 we generalized this molecular field approach for homopolymer melts to copolymer melts and described in detail its dielectric properties.

The conceptual point of the article is formulated in section 5: in the presence of an external field, it is not the simple composition f, but rather a more complicated object, an *effective composition*, is a relevant parameter of the problem. The essential conclusion is that, in an electric field, the composition, measured in numbers of statistical segments of blocks, cannot be defined unambiguously. Of course, the chemical composition f is the same with and without an electric field. However, the conformational and entropical properties of copolymers depend on the composition measured in numbers of Kuhn lengths rather than on the chemical composition. In an electric field, neither the Kuhn lengths of A and B units nor the associated composition of the copolymer can be defined unambiguously. That is why, for the electric field case, the composition f of the freely jointed model cannot participate, in some trivial way, in the free energy. This point is a keystone for understanding the features of the polymers in different fields.

This physical idea is realized within the framework of the random phase approximation in section 6. Unfortunately, the calculative procedure requires some casuistic mathematical steps and notions such as, for instance, the notion of quasi-noninteracting chains or an accurate separation of the full dipole moments into a spontaneously induced, strongly fluctuating part and a permanent part induced by an applied electric field. As it turned out, the electric field results only in an amusing rescaling of the space and a "renormalization" of the "bare" composition f. The simplest way to understand the effect of an electric field on a block copolymer is to examine the spinodal point and radiation scattering. The analysis (section 7) reveals that there are four universal classes of copolymer melt behavior in an electric field: $\mathcal{A}$, $\mathcal{B}$, $\mathcal{C}$, and $\mathcal{D}$. Each copolymer melt belongs to one of these classes, with a dependence upon three parameters, $S^{(A)}$, $S^{(B)}$, and f. $S^{(A)}$ and $S^{(B)}$ denote the birefringence of A and B blocks, respectively.

Each class has its specific X-ray pattern near the spinodal point and its specific dependence of the transition temperatures upon the applied electric field and reveals its specific cascade of phase transitions. These classes are described briefly in the abstract. A detailed calculation of the free energy, which permits the examination of the stability of different mesophases and prediction of phase transitions between them, is given in section 9. Classes $\mathcal{C}$ and $\mathcal{D}$ also reveal reentrant disorder → order → disorder or order → disorder → order phase transitions induced by the increasing field (section 10).

Increase of the electric field leads to the *orientational* transitions between different classes. For instance, a lamellar phase oriented perpendicularly to the electric field should be spontaneously transformed [by an *orientational* phase transitions smectic A (class $\mathcal{C}$) → smectic C (class $\mathcal{B}$) → smectic A (class $\mathcal{D}$)] into lamellar oriented parallel to the field. The orientational phase transitions are discussed in section 8.

In section 11 we discuss universal classes and their phase diagrams, industrial applications, and experimentally observable consequences of the theory. Nonessential mathematical details are summarized in Appendices.

2. Homopolymer Chain in an Electric Field

The conformation of a chain consisting of N repeat units is represented by the set of position vectors, $\{\vec{r}_K\}$, of the units ($K = 1, ..., N$) or alternatively as the set $\{\vec{a}_K = \vec{r}_{K+1} - \vec{r}_K\}$ of $N - 1$ bond vectors. The distribution function for the conformation of the freely jointed chain

is written as a product of distribution functions p for every unit

$$P(\{\vec{a}_K\}) = \prod_{K=1}^{N} p(\vec{a}_K) \tag{1}$$

For Gaussian chains the links have completely independent and random orientations: $p(\vec{a}_K)$ denotes the normalized random distribution of a vector of constant length a, and all the conformations have equal statistical weights. As a result, the probability $P_{IJ}(\vec{r}_I,\vec{r}_J)$ that the free jointed chain with the Ith unit at point $\vec{r}_I$ has the Jth unit at point $\vec{r}_J$ is a function of $r = |\vec{r}_I - \vec{r}_J|$ with a Fourier transform equal to[5,6]

$$P_{IJ}(\vec{Q}) = \exp\left(-x\frac{|I-J|}{N}\right) \tag{2}$$

$$x = \frac{Q^2Na^2}{6} = Q^2R^2$$

R^2 is called the mean square radius of gyration.

Conformation of an Ideal Chain in an Electric Field. An electric field, $\vec{E}$, polarizes segments, interacts with induced polar moments, and orients them. We consider an ideal homopolymer with the degree of polymerization N. The polar moment of the Kth unit, $\vec{P}_K$, is defined[8] as

$$(P_K)_i = \alpha_{ij}(\vec{a})E_j \tag{3}$$

where α_{ij} is the electric susceptibility (or polarizability) tensor of a link and $i,j = 1, 2, 3$. The linear dependence of a links dipole moment upon electric field intensity corresponds to the first term of the expansion of $\vec{P}_K$ in powers of $\vec{E}$ and is explained by the weakness of experimentally available fields by comparison with internal molecular fields. The polarizabilities along and perpendicular to the main axis of a unit are, generally speaking, different, and the induced dipole moment of a link depends upon its orientation with respect to electric field $\vec{E}$. In the case of rod-shaped segments (For more complicated symmetries case, see section 13 of ref 8 and section 37 of ref 9.), the polarizability tensor of the Kth unit is

$$\alpha_{ik}(\vec{a}) = \alpha\delta_{ik} + \nu\frac{a^i a^k}{a^2}$$

where δ_{ik} is the Kronecker δ function. The cases $\nu > 0$ and $\nu < 0$ correspond to the stronger polarizability along and perpendicular to the bond $\vec{a}_K$, respectively. It is usually convenient to decompose the polarizability tensor into an isotropic tensor and a purely anisotropic part with zero trace:

$$\alpha_{ik}(\vec{a}) = (\alpha + \nu/3)\delta_{ik} + \nu\left(\frac{a^i a^k}{a^2} - \frac{\delta_{ik}}{3}\right) \tag{4}$$

In polymeric systems, the anisotropic part is usually smaller than the isotropic part ($\nu/\alpha \leq 10^{-5}$).

The Hamiltonian H of a noninteracting chain described by a conformation $\vec{a}_K$ is represented as a sum of energies of N noninteracting dipoles in the electric field

$$H = -\sum_{K=1}^{K=N} \vec{E}\vec{P}_K \tag{5}$$

Since the polar moments depend on unit orientations, the chain energy in an electric field also depends upon chain conformation. Statistical weights differ for different conformations. The distribution function for chain conformations is

$$P(\{\vec{a}_K\}) = \exp\left(\frac{-H}{kT}\right)/Z$$

$$Z = \int \exp\left(\frac{-H}{kT}\right)\prod_{K=1}^{N} d\vec{a}_K$$

where T is the temperature and k is the Boltzmann constant. Due to the additivity of the chain energy (eq 5), the distribution function can be rewritten as a product (eq 1) of distribution functions, p, for each unit. Evidently, the segment distribution function, p, depends only upon the orientation dependent (or, in other words, anisotropic) part of the polarizability tensor, ν. Indeed (see Appendix A),

$$p(\vec{a}_K) = \exp\left(\frac{\nu(\vec{a}_K\vec{E})^2}{a^2kT}\right)/z \tag{6}$$

$$z = \int \exp\left(\frac{\nu(\vec{a}_K\vec{E})^2}{a^2kT}\right)d\vec{a}_K$$

For $\nu > 0$ ($\nu < 0$) the probability for a bond to be oriented along (perpendicular to) the electric field dominates. This results in a chain stretched or compressed, respectively, along the direction $\vec{E}$. This effect is known as intrinsic electric birefringence.[6,7]

The configuration of a chain is defined by the probability $P_{IJ}(\vec{r}_I,\vec{r}_J)$ that in the electric field the chain with the Ith unit at point $\vec{r}_I$ has the Jth unit at point $\vec{r}_J$. Using formulas 1 and 6 after a little bit of algebra (Appendix A) one obtains that P_{IJ} is a function of $r = |\vec{r}_I - \vec{r}_J|$ with the Fourier transform equal to

$$P_{IJ}(\vec{Q}) = \exp\left(-x\frac{|I-J|}{N}\right)$$

$$x = R^2(Q_l{}^2S + Q_p{}^2(3-S)/2) \tag{7}$$

where Q_l and Q_p are components of the wave vector directed along and perpendicular to an applied electric field, respectively, and the following notations are introduced:

$$S = 3\frac{\int_0^1 \zeta^2 e^{\xi\zeta^2}\,d\zeta}{\int_0^1 e^{\xi\zeta^2}\,d\zeta} \qquad \xi = \frac{\nu E^2}{kT} \tag{8}$$

Parameter ξ characterizes the tendency of an applied field to tilt segments disoriented by thermal fluctuations: kT is the thermal energy for one unit and νE^2 is the energy of a dipole in an electric field. Parameter S shown in Figure 1 describes the anisotropy of the chain deformed by the field. Its values range between 0 (for the negative anisotropic polarizability) and 3 (for the positive one).

Fourier transform of eq 7 gives the end-to-end distribution function in real space (Appendix B). If r_l and r_p denote the components of $\vec{r} = \vec{r}_I - \vec{r}_J$ along and perpendicular to $\vec{E}$, the probability $P_{IJ}(\vec{r})$ that the free

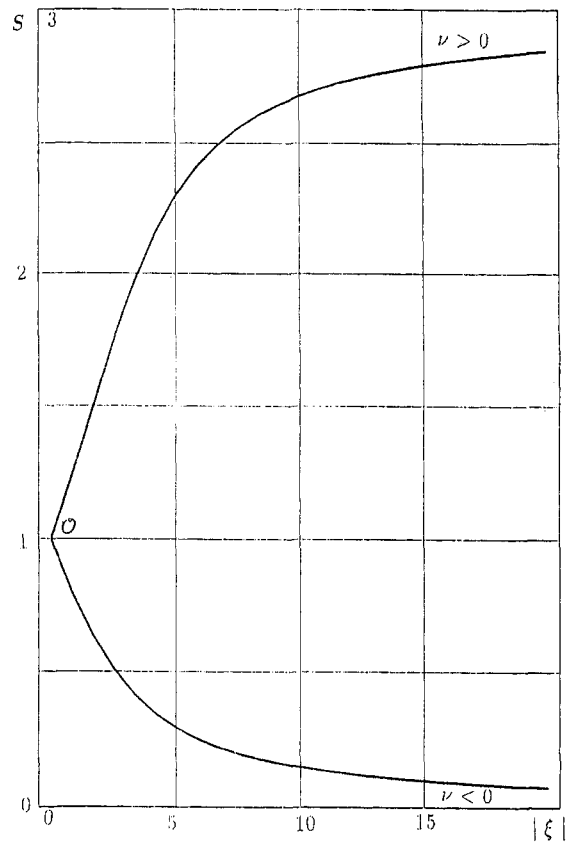

Figure 1. Parameter S of chain lengthening along the field vs $\xi = \nu E^2/kT$ for positive and negative anisotropic polarizability of segments, ν.

jointed chain with Ith unit at point $\vec{r}_I$ has the Jth unit at point $\vec{r}_J$ is proportional to

$$P_{IJ}(\vec{r}) \propto \exp\left(-\frac{3}{2}\frac{r_l^2}{|I-J|Sa^2}\right)\exp\left(-\frac{3}{2}\frac{2r_p^2}{|I-J|(3-S)a^2}\right) \quad (9)$$

The statistics of a chain with induced polar moment in an electric field is a quasi-Gaussian or axially deformed Gaussian statistics (compare expressions 7, 9, and 2).

Gyration Ellipsoid. If these coordinates are rescaled as follows,

$$r_l^2 \to r_l^2/S$$

$$r_p^2 \to 2r_p^2/(3-S) \quad (10)$$

the statistics (eq 7) of a chain in an electric field coincides with the statistics (eq 2) of an ideal Gaussian chain. For gyration radii along and perpendicular to an electric field $\vec{E}$, one automatically gets

$$R_l^2 = R^2S \qquad 2R_p^2 = R^2(3-S) \quad (11)$$

These radii define the size of the gyration ellipsoid in an applied electric field.

Dipole Moment of a Chain. The thermodynamically averaged induced dipole moment of a chain reads

$$\vec{P} = \int \sum_{K=1}^{K=N} \vec{P}_K \exp\left(\frac{\nu(\vec{a}_K\vec{E})^2}{a^2kT}\right) d\vec{a}_K/z \quad (12)$$

where the dipole moment of the Kth unit is given by eqs 3 and 4 and z is the normalizing coefficient. By symmetry, the full dipole moment of a free chain (a chain with nonfixed end-to-end vector) is directed along the field $\vec{E}$. Integration of the previous expression (Appendix A) gives

$$\vec{P} = (\alpha + \nu S(E)/3)N\vec{E} \quad (13)$$

The chain electric susceptibility is seen to be proportional to the degree of polymerization N and strongly depends upon the electric field intensity, E.

An expansion of the full dipole moment of a chain in powers of E includes only odd terms: indeed, the dipole moment must change its sign with inversion of the electric field ($\vec{E} \to -\vec{E}$ results in $\vec{P} \to -\vec{P}$). In the linear approximation in $\vec{E}$ (for a weak electric field) one finds an isotropically polarized Gaussian chain, $P = (\alpha + \nu/3)N\vec{E}$. In the limit of infinite electric field, all segments are oriented along E, and $P = (\alpha + \nu)N\vec{E}$. With increasing electric field, the chain is deformed, producing nonlinear dependence of polarizability upon electric field (see Appendix C). In order to prevent any misunderstanding, let us stress that the nonlinear polarizability of a chain arises only as a birefringence effect; the dipole moment of a link is a linear function of an applied electric field. Nonlinear behavior of a chain in an electric field appears only for anisotropically polarizable links.

Dipole–Dipole Interaction. The additivity of the full dipole moment as well as the quasi-Gaussian statistics (eq 7) of a chain in an electric field are not satisfied if dipole–dipole interactions are taken into account. Indeed, the energy of the dipole–dipole interaction[10] between the Ith unit at point $\vec{r}_I$ and the Jth unit at point $\vec{r}_J = \vec{r} + \vec{r}_I$ is

$$\frac{(\vec{P}_I\vec{P}_J)r^2 - 3(\vec{P}_I\vec{r})(\vec{P}_J\vec{r})}{r^3}$$

Summed over all pairs of chain segments, J and I, the dipole–dipole interaction contributes to the Hamiltonian (eq 5). The full chain energy is seen to become nonadditive: if the chain is divided into two parts, its energy cannot be presented as a sum of energies of each part, because of a dipole–dipole interaction between units belonging to different pieces. Similarly, the additivity of polarizability of a chain is lost.

For a chain in a solvent, this effect is called the form birefringence. It arises from the difference in dielectric constants of the region of a chain coil and of the matter around it. The form birefringence, a specific effect for the one chain system, is absent in homogeneous polymer melts.

3. Self-Consistent Approximation for a Homopolymer Melt in an Electric Field

In a concentrated melt considered as a continuous medium, as we will show, the dipole–dipole interaction taken into account does not change the additivity of the chain dipole moment or statistics (eq 6) of a chain. This follows directly from the symmetry properties of a chain with induced moments (see section 1). A quantitative description of chain statistics in a polymeric melt demands a more detailed analysis.

The real electric forces acting on a segment in a melt include the electric forces of its interaction with all the polarized units of the system as well as the external electric forces of the experimental setup. In order to account for the dipole–dipole interaction, let us consider

the field $\vec{E}$ in the Hamiltonian (eq 5) as a real internal electric field in the melt. This field, defined by a temporal and spatial averaging of the microscopic electric field, is a sum of the external (experimentally applied) electric field, $\vec{\mathcal{E}}$ and the field due to all other dipoles of the melt. Formula 13 of section 2 is the correct expression for chain polarization in terms of the internal electric field. Similarly, the configuration of a chain in the melt as a function of the internal electric field is given by eqs 7 and 9.

However, measurements of polarization $\vec{P}$ are usually made by measuring the capacitance of a capacitor as a function of the external field. To exploit the results, a theory is required relating the internal electric field, $\vec{E}$, to the external applied field, $\vec{\mathcal{E}}$. This relation includes, generally speaking, polarization ($\vec{P}/Nv$) of the unit volume of a copolymer melt through the so-called dipolarizator factor.[10] The only problem is that the dipolarizator factor depends upon the concrete geometry of the experiment.

For a thin macroscopic slab of a polymer melt oriented with long dimension parallel to the applied electric field:

$$\vec{E} = \vec{\mathcal{E}} \tag{14}$$

In such a case the dipole moment per chain is given by the substitution of $\vec{\mathcal{E}}$ for $\vec{E}$ in expression 13

$$P = (\alpha + \nu S(\mathcal{E})/3)N\mathcal{E} \tag{15}$$

However, the most common experimental arrangement is a thin (but macroscopic) slab of a polymer melt placed in the vacuum between plates of a capacitator perpendicular to the applied electric field.[3] In such a case, the internal electric field as a function of the chain polarization reads[10]

$$\vec{E} + \frac{4\pi}{v}\frac{\vec{P}}{N} = \vec{\mathcal{E}} \tag{16}$$

where $\vec{P}$ is the dipole moment of a chain as a function of the internal field given by eq 13, N is the degree of polymerization, and v is the volume per segment. P/Nv is polarization moment per unit volume of the polymer melt and $E + 4\pi P/Nv$ is the induction vector of the electric field. When the polarization, P, is eliminated from formulas 13 and 16, we obtain a self-consistent equation,

$$E + \frac{4\pi}{v}\{\alpha + \nu S(E)/3\}E = \mathcal{E} \tag{17}$$

for the internal electric field E in a polymer melt. This equation can be solved numerically or by expansion of the internal field E in powers of the applied field $\mathcal{E}$. (In order to compare our predictions with experiments, the expansion is written out in Appendix C.)

For other geometries of experimental setups, the relation between the electric field inside and outside the melt are written out in ref 8, sections 4, 8.

Let us summarize the results. In a homogeneous melt the statistics of chains is quasi-Gaussian (eq 7). The chain polarization, $\vec{P}$ (proportional to the degree of polymerization, N), behaves nonlinearly with respect to the electric field. The parameter of stretching, S, and the dipole moment of a chain, P, are given explicitly in terms of the internal electric field, E, which is related by eqs 14 and 17 to an applied external electric field, $\mathcal{E}$.

4. A Self-Consistent Approximation for a Copolymer Melt in an Electric Field

The notion of a noninteracting ideal (or Gaussian) chain is a conceptional one for the physics of polymer melts. In copolymer melts, it may be supposed that when interactions between monomers of different chemical nature are switched off the distribution functions of chains are equal to those of the Gaussian (noninteracting) copolymer chains. In an applied electric field, the notion of a system of noninteracting copolymer chains has to be revised and clarified.

Diblock Conformation in an Electric Field. Quasi-Noninteracting Chains. In a copolymer melt, the intermolecular forces acting on a unit are of three different types: firstly, one which provides the constant density of segments; secondly, an effective interaction between units of different nature (the so-called Flory–Huggins interaction); and, thirdly, a dipole–dipole interaction between units polarized by the electric field. The first two forces are local: they act on scales of the statistical segment length. The dipole–dipole interaction is a long-range one. It contributes to birefringence and crucially changes chain conformations. We will consider below a copolymer melt with the local interaction between units of different nature switched off, but take into account the long-range dipole–dipole interaction. Thus, we will consider below quasi-noninteracting (do not forget about the dipole–dipole interaction) chains, i.e., a homogeneous copolymer melt of a constant over-all density with long-range dipole-dipole interactions between units polarized by the electric field.

A self-consistent theory of homogeneous melts in an electric field was developed in section 3. The internal electric field ($\vec{E}$) which arises in the volume of a melt polarizes segments. The dipole moment per repeat units is

$$(P)_k^{(i)} = \alpha_{kj}^{(i)}(\vec{a})E_j,$$

where the indices (i), where i = A, B, correspond to A and B units, respectively. Polarizability tensors of A and B links depend on the orientation, $\vec{a}$

$$\alpha_{ik}^{(i)}(\vec{a}) = (\alpha^{(i)} + \nu^{(i)}/3)\delta_{ik} + \nu^{(i)}\left(\frac{a_i a_k}{a^2} - \frac{\delta_{ik}}{3}\right)$$

A procedure of measuring α and ν polarizability coefficients in homopolymer melts is discussed in detail in section 3.

Gyration Ellipsoids of Blocks. In the self-consistent approximation for an electric field, the conformations of A and B blocks are seen to be independent. As a result, the end-to-end vector of a diblock, $\vec{R}$, is equal to the sum of the end-to-end vectors (eq 11) of blocks:

$$\vec{R} = \vec{R}^{(A)} + \vec{R}^{(B)} \tag{18}$$

For gyration radii of A and B blocks along and perpendicularly to an applied electric field, R_l and R_p, one has

$$(R_l^{(A)})^2 = (R^{(A)})^2 S^{(A)}$$

$$2(R_p^{(A)})^2 = (R^{(A)})^2(3 - S^{(A)})$$

$$(R^{(A)})^2 = R^2 f$$

and

$$(R_l^{(B)})^2 = (R^{(B)})^2 S^{(B)}$$

$$2(R_p^{(B)})^2 = (R^{(B)})^2(3 - S^{(B)})$$

$$(R^{(B)})^2 = R^2(1-f)$$

respectively. We introduced the following notations

$$S^{(i)} = 3\frac{\int_0^1 \zeta^2 e^{\xi^{(i)}\zeta^2}\,d\zeta}{\int_0^1 e^{\xi^{(i)}\zeta^2}\,d\zeta} \qquad \xi^{(i)} = \frac{\nu^{(i)}E^2}{kT}$$

A rigorous calculation of the gyration ellipsoids sizes is given in Appendix B.

In spite of the dipole–dipole interaction between units, the distribution functions $p(\vec{a}_K)$ of units were shown to be independent (but different, of course, from those of randomly oriented units in the ideal Gaussian chain). For a diblock chain with the composition f, the distribution of its conformations is written as a product of distribution functions for every unit

$$P_{IJ}(\{\vec{a}_K\}) = \prod_{K=I}^{J} p(\vec{a}_K) =$$

$$= \prod_{K=I}^{Nf} p(\vec{a}_K) \prod_{K=Nf}^{J} p(\vec{a}_K)$$

Here $p(\vec{a}_K)$ is the distribution function of the Kth unit. The probability, $P_{IJ}(\vec{r}_I,\vec{r}_J)$, to have the Ith unit at point $\vec{r}_I$ and the Jth unit at point $\vec{r}_J$ is (after Fourier transformation)

$$P_{IJ}(\vec{Q}) = P_{IJ}^{(A)}(\vec{Q}) \qquad I, J < Nf$$

$$P_{IJ}(\vec{Q}) = P_{INf}^{(A)}(\vec{Q})P_{NfJ}^{(B)}(\vec{Q}) \qquad I < Nf < J \quad (19)$$

$$P_{IJ}(\vec{Q}) = P_{JNf}^{(A)}(\vec{Q})P_{Nfl}^{(B)}(\vec{Q}) \qquad J < Nf < I$$

$$P_{IJ}(\vec{Q}) = P_{IJ}^{(B)}(\vec{Q}) \qquad Nf < I, J$$

The functions $P_{IJ}^{(i)}$ given above by eq 7 are as follows

$$P_{IJ}^{(i)}(\vec{Q}) = \exp\left(-x^{(i)}\frac{|I-J|}{N_{(i)}}\right) \quad (20)$$

with

$$fx^{(A)} = (Q_l R_l^{(A)})^2 + (Q_p R_p^{(A)})^2$$

$$(1-f)x^{(B)} = (Q_l R_l^{(B)})^2 + (Q_p R_p^{(B)})^2 \quad (21)$$

where Q_l, R_l and Q_p, R_p are components of wave vectors and gyration radii along and perpendicular to the applied electric field, respectively. Copolymer chain (eq 19) consists of two A and B blocks differently deformed by the field. The birefringence depends only upon the anisotropic part of the segment polarizability tensors, $\nu^{(A)}$ and $\nu^{(B)}$. For isotropically polarizable links, the conformation of chains in an electric field coincides with that of an ideal Gaussian chain.

Dipole Moment of a Copolymer. The full dipole moment (eq 12) of a copolymer chain is proven to be an additive function: when the chain is divided into parts, the total dipole moment equals to the sum of both moments. The full dipole moment of a diblock as a function of the internal electric field, $\vec{E}$, is

$$\vec{P} = (\alpha^{(A)} + \nu^{(A)}S^{(A)}/3)fN\vec{E} +$$

$$(\alpha^{(B)} + \nu^{(B)}S^{(B)}/3)(1-f)N\vec{E} \quad (22)$$

To exploit this result, one is required to relate the internal electric field, $\vec{E}$, to the applied field, $\vec{\mathcal{E}}$. The dipole–dipole interaction (as well as an applied external field $\vec{\mathcal{E}}$) contributes to the internal field, $\vec{E}$. For a thin slab of a copolymer (eq 3) oriented perpendicular to an applied electric field, $\mathcal{E}$, this relation is

$$\mathcal{E} = E + \frac{4\pi}{v}(\{\alpha^{(A)} + \nu^{(A)}S^{(A)}(E)/3\}f +$$

$$\{\alpha^{(B)} + \nu^{(B)}S^{(B)}(E)/3\}(1-f))E \quad (23)$$

where v is a volume per segment. (One gets eq 23 by a straightforward substitution of eq 22 into electrostatic relation 16.) Nonlinear integral relation 23 between applied and internal electric fields arises from the dipole–dipole interaction. The solution of this equation for the internal electric field $E = E(\mathcal{E})$ substituted in formula 22 provides the copolymer chain birefringence and its dipole moment as functions of the applied electric field, $\mathcal{E}$, in homogeneous copolymer melts.

5. Effective Composition

For the freely jointed chain, the composition, f, is defined as the ratio of a number of A units (statistical segments A (N_A) to the full number ($N_A + N_B$) of units (statistical segments). Thus, for a Gaussian chain, one has

$$\frac{(R^{(A)})^2}{(R^{(B)})^2} = \frac{f}{1-f}$$

where the statistical lengths of A and B units are being taken as equal.

Electric field does not change the numbers of A and B units in a chain. However, the conformational and entropic properties of copolymers depend upon the composition measured in numbers of Kuhn lengths rather than upon the chemical composition. The electric field orients segments and the stiffness of a chain is different along and perpendicular to $\vec{E}$. The statistical properties of a chain at a given point $\vec{r}$ depend upon the local orientation of the chain with respect to electric field. Neither the Kuhn length nor an associated with "composition" can be defined.

Indeed, an effective compositions, $\tilde{f}$, associated with and measured in Kuhn lengths along and perpendicular to $\vec{E}$, f_*^* and f_*^{**}, are different.

$$\frac{f_*^*}{1-f_*^*} = \frac{(R_l^{(A)})^2}{(R_l^{(B)})^2} = \frac{f}{1-f}\frac{S^{(A)}}{S^{(B)}}$$

$$\frac{f_*^{**}}{1-f_*^{**}} = \frac{(R_p^{(A)})^2}{(R_p^{(B)})^2} = \frac{f}{1-f}\frac{(3-S^{(A)})}{(3-S^{(B)})}$$

As seen, in an electric field, the composition measured the numbers of statistical segment of A and B blocks is an unambiguously defined variable. The main point of the current theory is that for oriented (by electric, shear, or liquid crystalline fields) segments, it is not the simple composition, f, but rather a more complicated object, an *effective composition*, that is a relevant parameter of the problem.

The statistical segment can be defined for any arbitrary chosen direction, for instance, $\vec{Q}$. The diblock effective composition, $\tilde{f}$, measured in Kuhn lengths associated with direction $\vec{Q}$ is

$$\frac{\tilde{f}(\vec{Q})}{1-\tilde{f}(\vec{Q})} = \frac{(R_l^{(A)}Q_l)^2 + (R_p^{(A)}Q_p)^2}{(R_l^{(B)}Q_l)^2 + (R_p^{(B)}Q_p)^2} \tag{24}$$

The notion of the effective composition is a keystone for an understanding of phenomena induced by fields in complex polymeric liquids.

6. Free Energy of Molten Block Copolymers in an Electric Field

In this section we generalize the random phase approximation developed by Leibler to the case with an electric field. The random phase approximation[4] provides the relation of the free energy of a melt to the response functions of Gaussian noninteracting chains. We relate the free energy of the system to the response functions of those copolymer chains for which the long-range dipole–dipole interactions between links and their interaction with an applied electric field are taken self-consistently into account. We sketch and review here some essential points of ref 4 which are necessary for the reader to follow our further logic.

Random Phase Approximation for Microphase Separation. The picture of microphase separation given by Leibler[4] was based on several assumptions. The statistical lengths of A and B links are assumed to be equal. The full number of monomers per unit volume (ϱ) was considered to be a constant. Due to this last (incompressibility) condition, the deviation of the A units density, ϱ_A, at point $\vec{r}$ from the uniform distribution value completely describes weakly ordered states and can be treated as an order parameter. For copolymers of composition f, the order parameter is

$$\psi(\vec{r}) = \frac{\varrho_A(\vec{r})}{\varrho} - f.$$

The free energy per chain can be presented as a Landau expansion in the order parameter. Up to the fourth-order term in the order parameter, it reads

$$\frac{F(\psi)N}{kT} = \frac{N}{2!}\int(\Gamma_2 - 2\chi)\prod_{n=1}^{2}\psi(\vec{Q}_n)\frac{d^3Q_n}{(2\pi)^3} + \frac{N}{3!}\int\Gamma_3\prod_{n=1}^{3}\psi(\vec{Q}_n)\frac{d^3Q_n}{(2\pi)^3} + \frac{N}{4!}\int\Gamma_4\prod_{n=1}^{4}\psi(\vec{Q}_n)\frac{d^3Q_n}{(2\pi)^3} \tag{25}$$

where N and χ are, respectively, the degree of polymerization and the Flory–Huggins interaction parameter, and the $\psi(\vec{Q})$'s are Fourier components of the order parameter.

In eq 25 the term $\chi\psi^2$ describes the Flory–Huggins interaction between A and B units. Units A and B effectively always repeal each other. The origin of the repulsion between units of different chemical nature lies in a short-range dipole–dipole interaction between links mutually spontaneously polarized.[15] All other terms in expansion 25 describe the contribution to the free energy from the loss of the configurational entropy of ordered copolymer chains.

The local Flory–Huggins interaction having been taken into account, all other terms in the energy expansion can be calculated by an approximation as if the interaction χ between units is switched off. This is the so-called random phase approximation. The vertices Γ_2, Γ_3, Γ_4 are wave vector dependent functions, which may be expressed in terms of two-, three- and four-monomer density correlators, $G_{ij}^{(2)}$, $G_{ijk}^{(3)}$, $G_{ijkl}^{(4)}$ ($i, j, k, l = 1, 2$), as

$$\Gamma_2(f) = G_{ij}^{(2)}(\vec{Q}_1,\vec{Q}_2)\{G_{i1}^{-1}(\vec{Q}_1) - G_{i2}^{-1}(\vec{Q}_1)\} \times \{G_{j1}^{-1}(\vec{Q}_2) - G_{j2}^{-1}(\vec{Q}_2)\} \tag{26}$$

$$\Gamma_3(f) = -G_{ijk}^{(3)}(\vec{Q}_1,\vec{Q}_2,\vec{Q}_3)\{G_{i1}^{-1}(\vec{Q}_1) - G_{i2}^{-1}(\vec{Q}_1)\} \times \{G_{j1}^{-1}(\vec{Q}_2) - G_{j2}^{-1}(\vec{Q}_2)\}\{G_{k1}^{-1}(\vec{Q}_3) - G_{k2}^{-1}(\vec{Q}_3)\}$$

$$\Gamma_4(f) = \gamma_{ijkl}(\vec{Q}_1,\ldots,\vec{Q}_4)\{G_{i1}^{-1}(\vec{Q}_1) - G_{i2}^{-1}(\vec{Q}_1)\} \times \{G_{j1}^{-1}(\vec{Q}_2) - G_{j2}^{-1}(\vec{Q}_2)\}\{G_{k1}^{-1}(\vec{Q}_3) - G_{k2}^{-1}(\vec{Q}_3)\}\{G_{l1}^{-1}(\vec{Q}_4) - G_{l2}^{-1}(\vec{Q}_4)\}$$

where G_{ij}^{-1} is the (ij) component of the matrix inverse of the matrix $G_{ij}^{(2)}$ and

$$\gamma_{ijkl}(\vec{Q}_1,\vec{Q}_2,\vec{Q}_3,\vec{Q}_4) = \sum_{\vec{Q}} G_{mn}^{-1}(\vec{Q})\{G_{ijm}^{(3)}(\vec{Q}_1,\vec{Q}_2,\vec{Q}) \times G_{nkl}^{(3)}(-\vec{Q},\vec{Q}_3,\vec{Q}_4) + G_{ikm}^{(3)}(\vec{Q}_1,\vec{Q}_3,\vec{Q})G_{njl}^{(3)}(-\vec{Q},\vec{Q}_2,\vec{Q}_4) + G_{ilm}^{(3)}(\vec{Q}_1,\vec{Q}_4,\vec{Q})G_{nkj}^{(3)}(-\vec{Q},\vec{Q}_3,\vec{2})\} - G_{ijkl}^{(4)}(\vec{Q}_1,\vec{Q}_2,\vec{Q}_3,\vec{Q}_4)$$

Equations 26 follow from very general relations between the order parameter correlators and the vertices in the energy expansion.[12]

When the effective repulsion between A and B units is switched off, the conformation of a copolymer chain in the melt is described by Gaussian statistics of an ideal noninteracting chain. Chains are statistically independent and monomer–monomer correlation functions $G_{ij}^{(2)}$, $G_{ijk}^{(3)}$, and $G_{ijkl}^{(4)}$, ($i, j, k, l = 1, 2$) may be expressed solely in terms of one-chain correlators, $P_{IJK\ldots}(\vec{r}_I,\vec{r}_J,\vec{r}_K\ldots)$, which denote the probability that a chain with the Ith unit at point $\vec{r}_I$ has the Jth unit at point $\vec{r}_j$ and the Kth unit at point $\vec{r}_K$ and so on. In turn, all one-chain probabilities $P_{IJK\ldots}$ for Gaussian chains are written as a products of pair probabilities P_{IJ}. For instance, if $I > J > K$,

$$P_{IJK}(\vec{Q}) = P_{IJ}(\vec{Q})P_{JK}(\vec{Q})$$

One finally gets that all the monomer–monomer correlators depend only upon the pair correlator P_{IJ}:

$$G_{ij}^{(2)} = G_{ij}^{(2)}(P_{IJ}) \qquad G_{ijk}^{(3)} = G_{ijk}^{(3)}(P_{IJ}) \qquad G_{ijkl}^{(4)} = G_{ijkl}^{(4)}(P_{IJ}) \tag{27}$$

For example, a contribution to the correlator $G_{112}^{(3)}$ is [see ref 4, Appendix C, (C-1)]

$$\int_{fN}^{N} dI \int_0^{fN} dJ \int_0^{J} dK\, P_{IJ}(\vec{Q})P_{JK}(\vec{Q}) \tag{28}$$

Similar integrations give other high-order response functions also in terms of $P_{IJ}(\vec{Q})$. The interested reader should consult ref 4 for all the calculative details of G-functions.

As χN is increased, a competition between the repulsion energy of incompatible links (the term proportional to χN) and the configurational entropy of chains (all the

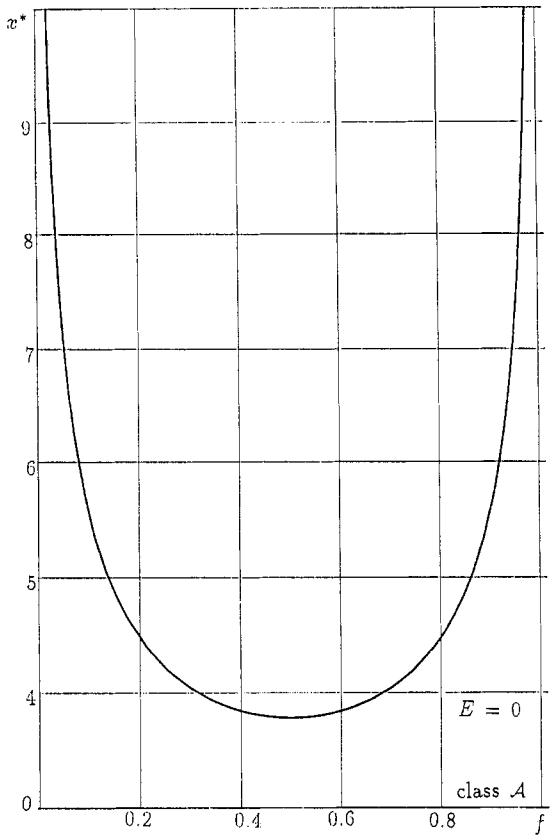

Figure 2. The equilibrium periodicity parameter, $x^* = Q^{*2}R^2$, vs composition f in the absence of an electric field.[4] It gives the size of the sphere of the critical wave vectors in Q-space (in units of squared gyration radius in zero electric field). The equilibrium periodicity parameter $\tilde{x}$ vs composition f in applied field for a copolymer melt of class A (see section 7, eq 38). It gives the size of the ellipsoid formed by the critical wave vectors in Q-space (in units of squared gyration radius in zero electric field, R^{-2}).

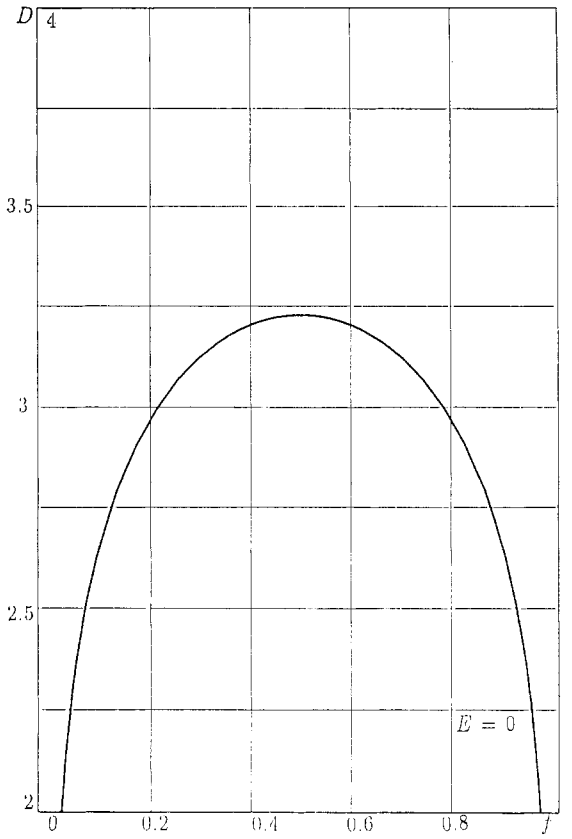

Figure 3. The periodicity, D, of the structure vs f in the absence of an electric field (in units of gyration radius in zero electric field).

other addings) produces the order–disorder transition. The value

$$x^* = (Q^*)^2R^2 \tag{29}$$

corresponding to the minimum of $\Gamma_2(f,x)$ gives a periodicity $2\pi/Q^*$ of the ordered structures as functions of the composition f. A remakable property of molten copolymers is that x^* is independent of the interaction parameter χ. Dependencies of x^* and the periodicity, D, of the structure just after microphase separation vs f are shown in Figures 2 and 3. In Q-space, equation 29 defines a sphere of critical wave-vectors Q^*: as χN reaches the spinodal value, $(\chi N)_c$, the fluctuations with wave vector, $|q| = Q^*$, diverge.

The spinodal line, $(\chi N)_c$, is

$$(\chi N)_c = \Gamma_2(f,x^*) \tag{30}$$

Due to the fact that the equilibrium value of the periodicity parameter, x^*, depends only upon the composition, f, the spinodal line (eq 30) is also a universal function of the composition (Figure 4).

Upon increasing χN (or asymmetry of a chain) a disordered melt → body-centered cubic → hexagonal → lamellar cascade of first-order transitions occurs. The only relevant value for the phase diagram parameters turn out to be the product χN and the fraction f of units A in a chain. For symmetric diblocks, the transition from molten to lamellar phase was found to be continuous. The corresponding phase diagram for diblocks is shown in Figure 5.

Random Phase Approximation for an Electric Field. In an electric field the intermolecular dipole interactions in copolymer melts are of two different types. The first one is a dipole–dipole interaction between spontaneously induced dipoles, $\vec{\mathcal{R}}$, of segments. In fact, this is the Flory–Huggins interaction, χ. This interaction, which results in the effective repulsion of A and B units, is local: it acts and strongly fluctuates on molecular times and scales. Over a distance of several statistical lengths, this interaction is completely screened (that is why the Flory–Huggins term in the free energy expansion is local). Molecular electric fields and dipole moment, $\vec{\mathcal{R}}$, cannot be considered as objects of a thermodynamic description, since after statistical averaging all nontrivial correlators of spontaneously induced dipoles, $\vec{\mathcal{R}}$, equal zero

$$\langle\vec{\mathcal{R}}(\vec{r}_I)\rangle = 0$$

$$\langle\vec{\mathcal{R}}(\vec{r}_I)\vec{\mathcal{R}}(\vec{r}_J)\rangle = \langle\vec{\mathcal{R}}(\vec{r}_I)\rangle\langle\vec{\mathcal{R}}(\vec{r}_J)\rangle = 0$$

$$\langle\vec{\mathcal{R}}(\vec{r}_I) \ldots \vec{\mathcal{R}}(\vec{r}_J)\rangle = \langle\vec{\mathcal{R}}(\vec{r}_I)\rangle \ldots \langle\vec{\mathcal{R}}(\vec{r}_J)\rangle = 0$$

if only $\vec{r}_I \neq \vec{r}_J$. They, therefore, cannot enter macroscopic thermodynamics. This local dipole–dipole interaction is introduced phenomenologically through the Flory–Huggins parameter, χ.

The other part of the molecular interaction is an interaction between dipoles, $\vec{P}$, induced by an applied field. This long-range (in principal infinite-range) interaction contributes to birefringence effects and changes the entropy of deformed copolymer chains. This interaction is an object of a thermodynamic description (sections 3, 4). It results in the fact that in melts the macroscopical internal electric field, E, differs from the external applied electric field, $\mathcal{E}$.

The essential physical point is that these two dipole–dipole interactions are separated and do not interfere.

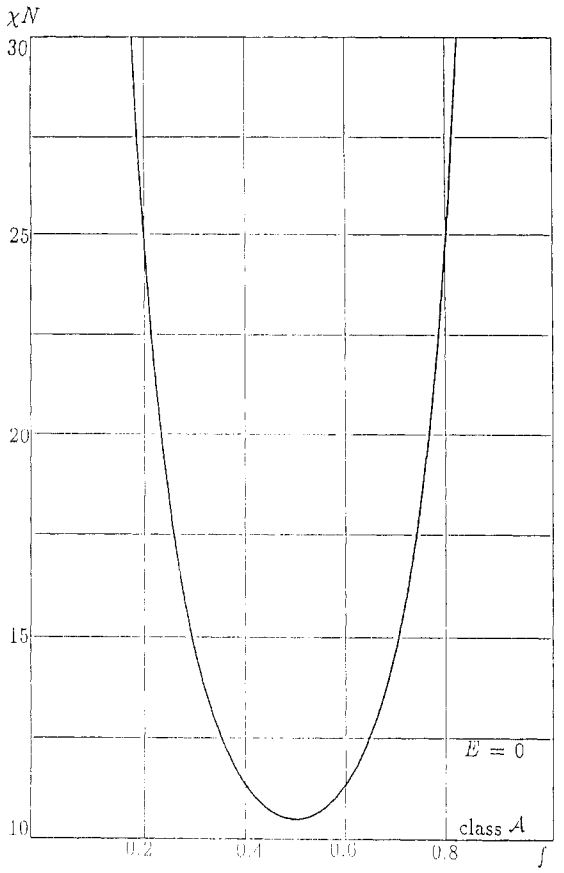

Figure 4. The spinodal point vs composition f in the absence of an electric field.[4] The spinodal point vs f for a copolymer melt of class A in an electric field. The spinodal point for class A is a universal function solely of f: it does not depend on an electric field and coincides with the spinodal point in zero electric field.

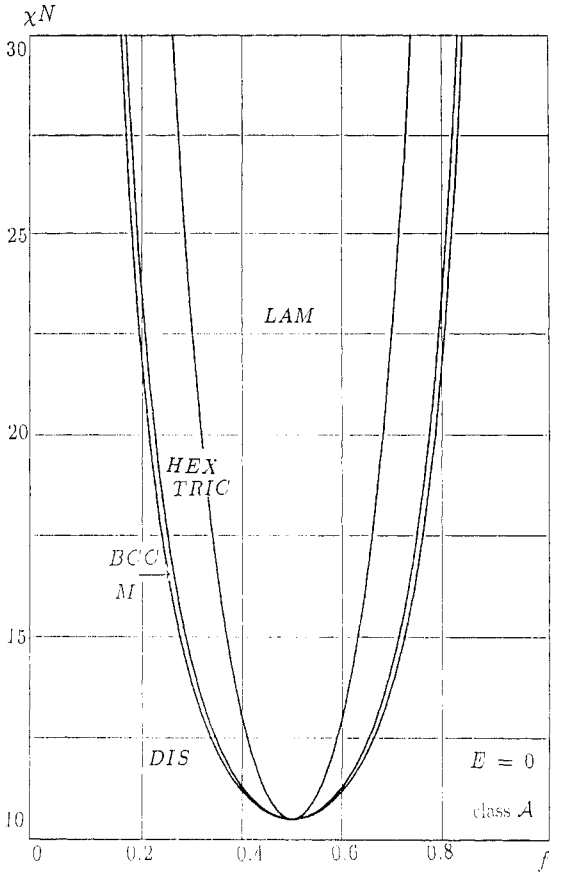

Figure 5. Phase diagram[4] for a copolymer melt in the absence of an electric field. It presents the region of stability of body-centered-cubic, hexagonal, and lamellar phases in the plane with coordinates f and χN. Phase diagram for a diblock copolymer melt of class A. It presents the stability regions of a three-dimensional monoclinic, a two-dimensional triclinic and a one-dimensional lamellar phases. The temperatures of these weak first-order transitions do not depend on the field intensity, E.

Indeed, experimentally available electric fields are too weak ($E < 10^7\ V\ m^{-1}$) in comparison with fluctuational molecular electric fields to change microscopic polarizability tensors of segments. So, the Flory–Huggins interaction parameter, χ, is unchanged in an electric field. On the other hand, a spontaneous dipole moment, $\vec{\mathcal{R}}$, which fluctuates on molecular times, does not contribute to the permaent dipole moment, $\vec{P}_J$, of a link. The thermodynamically averaged energy of the dipole–dipole interaction[10] between the Ith and the Jth units at positions $\vec{r}_I$ and $\vec{r}_J = \vec{r} + \vec{r}_I$ is split into two independent parts:

$$\left\langle \frac{(\vec{P}_I + \vec{\mathcal{R}}_I)(\vec{P}_J + \vec{\mathcal{R}}_I)}{r} \right\rangle - 3\left\langle \frac{((\vec{P}_I + \vec{\mathcal{R}}_I)\vec{r})((\vec{P}_J + \vec{\mathcal{R}}_J)\vec{r})}{r^3} \right\rangle = \frac{\vec{P}_I\vec{P}_J r^2 - 3(\vec{P}_I\vec{r})(\vec{P}_J\vec{r})}{r^3} + \frac{\langle \vec{\mathcal{R}}_I\vec{\mathcal{R}}_J\rangle r^2 - 3\langle(\vec{\mathcal{R}}_I\vec{r})(\vec{\mathcal{R}}_J\vec{r})\rangle}{r^3}$$

The last term on the right-hand side of this equation is nonzero only if $r = 0$ and contributes to the local Flory–Huggins effective interaction. The first term contributes to the electrostatic energy and leads to a birefringence. Thus, in an electric field, the Flory–Huggins interaction and the dipole–dipole interaction between induced polar moments of links contribute separately to the free energy.

Let us extract from the full free energy the energy of local interactions: the Flory–Huggins interaction, $\chi\psi^2$, and a part of the electrostatic energy[3,14] related to space modulations of the internal field, $(\alpha^{(A)} - \alpha^{(B)})^2\mathcal{E}^2\psi^2$. As it was explained before, the Flory–Huggins coefficient χ is of the order of $(\alpha^{(A)} - \alpha^{(B)})^2\mathcal{F}^2$, where $\mathcal{F}$ is the strongly fluctuating molecular electric field. Since experimentally available electric fields, $\mathcal{E}$, are 100 times smaller than molecular fields, $\mathcal{F}$, the electrostatic corrections below will be neglected. In principal, they could lead to a shift of χ.

Once the energy of local monomer–monomer interactions (the energy of the "broken-link" system[13] are extracted in eq 25, all the other terms in the free energy expansion describe a loss of the configurational entropy. We will develop below the random phase approximation based on the statistics (eq 19) of quasi-noninteracting chains: For the local internal electric field, $E(\vec{r})$, we substitute the space averaged internal electric field calculated at the spinodal point, i.e., we neglect the phenomenon of the form birefringence (section 2). This simplification implies that (in the vicinity of the spinodal point) the difference in polarizabilities of A and B segments, $\nu^{(A)}$ and $\nu^{(B)}$, is more essential than a difference coming from space modulations of the internal electric field (for the discrimination in the statistics of blocks). In the absence of the dipole–dipole interaction between induced polar moments, the internal electric field, E, coincides with the applied external field, $\mathcal{E}$, and our approximative picture becomes exact.

By using the statistics (eqs 19 and 20) of quasi-noninteracting chains, which take into account the dipole–dipole interaction of the polarized units, we relate the coefficients of the expansion of the configurational entropy in powers of ψ to the response functions of the order parameter (see ref 11, sections 5.4, 5.5)) at the spinodal point. Relations 26 apply for any bicom-

ponent system if only the constant overall density condition is provided, in particular, for a copolymer melt in an electric field.

The statistics of quasi-noninteracting copolymer chain in an electric field are nonGaussian statistics. But chains are independent and monomer–monomer correlators $G^{(n)}_{ijkl...}(E)$ in an electric field may be expressed solely in terms of one-chain probabilities $P_{IJK...}(E)$. The probabilities $P_{IJK}(E)$ are written as products of the pair correlators $P_{IJ}(E)$, in the same way as for Gaussian ideal chains, in spite of the fact that A and B blocks are differently deformed. This means that expressions 27 of response functions $G^{(n)}_{ijkl...}$ for ideal Gaussian chains in terms of the probability $P_{IJ}(\bar{r})$ apply directly to the electric field case: one has only to substitute in eq 27 the pair, correlator $P_{IJ}(E)$ of a quasi-noninteracting copolymer chain (eq 19) for the pair correlator P_{IJ} of an ideal chain (eq 2). For example, a contribution to the third-order response functions $G^{(3)}_{112}(E)$ in an electric field is

$$\int_{fN}^{N} dI \int_{0}^{fN} dJ \int_{0}^{J} dK\, P_{IJ}(E,Q)P_{JK}(E,Q)$$

(Compare with expression 28.)

Nonlinear Response Functions of Copolymers in an Electric Field. A straightforward calculation of the nonlinear response functions G would require very formidable algebra. Indeed, the response functions of copolymer chains in an electric field depend on the composition, f, the degree of polymerization, N, the anisotropic parts of the A and B unit susceptibilities, $\nu^{(A)}$ and $\nu^{(B)}$, kT, and the internal electric field, $\vec{E}$ (which in turn has a nonlinear integral relation to the experimentally applied field, $\vec{\mathcal{E}}$). However, one can escape calculations of the nonlinear response functions, if the reader will have sufficient patience to follow the reasoning of Appendix D. The result reads as follows: an nth-order response function in an electric field

$$G^{(n)}_{i_1 i_2 \ldots i_n}(E)$$

$$\underbrace{i_l, i_m \ldots = 1}_{p} \qquad \underbrace{i_k, i_l, \ldots = 2}_{n-p}$$

having p indices 1 (which correspond to A units) and $n - p$ indices 2 (which correspond to B units) is obtained by substitutions into the corresponding response function $G^{(n)}_{i_1 i_2 \ldots i_n}$ of an ideal Gaussian chain as follows:

$$e^{xf} \to e^{x^{(A)}f}$$

$$e^{x(1-f)} \to e^{x^{(B)}(1-f)}$$

$$x^n \to (x^{(A)})^p (x^{(B)})^{n-p} \tag{31}$$

where $x^{(A)}$ and $x^{(B)}$ are given by eq 20. For instance, the third-order response function[4]

$$G^{(3)}_{112}(h,f) = \frac{2N^2}{x^3}(1 - e^{-x(1-f)h})\left(\frac{1}{h} - \frac{e^{-xf}}{1-h} + \frac{e^{-xfh}}{h^2 - h}\right)$$

of Gaussian chains with the degree of polymerization N and the composition f is

$$\frac{2N^2}{x^{(A)2}x^{(B)}}(1 - e^{-x^{(B)}(1-f)h})\left(\frac{1}{h} - \frac{e^{-x^{(A)}f}}{(1-h)} + \frac{e^{-x^{(A)}fh}}{h^2 - h}\right)$$

in the case of a nonzero electric field.

Trick of a Composition Renormalization and a Rescaling of Space. The last step is to introduce a new periodicity parameter $\tilde{x}$ and a new "effective composition", $\tilde{f}$, defined as follows:

$$\tilde{x}\tilde{f} = x^{(A)}f \qquad \tilde{x}(1-\tilde{f}) = x^{(B)}(1-f) \tag{32}$$

The effective composition, $\tilde{f}$, and the periodicity parameter, $\tilde{x}$, depend on the applied electric field and are functions of a wave vector, $\vec{Q}$. With these variables, transformation rules 31 read

$$e^{x(1-f)} \to e^{\tilde{x}(1-\tilde{f})} \qquad e^{xf} \to e^{\tilde{x}\tilde{f}}$$

$$x^n \to \tilde{x}^n \left(\frac{\tilde{f}}{f}\right)^p \left(\frac{1-\tilde{f}}{1-f}\right)^{n-p}$$

For response functions in an electric field one finally gets

$$G^{(n)}_{i_1 i_2 \ldots i_n}(E) = \left(\frac{\tilde{f}}{f}\right)^p \left(\frac{1-\tilde{f}}{1-f}\right)^{n-p} G^{(n)}_{i_1 i_2 \ldots i_n}(\tilde{x},\tilde{f}) \tag{33}$$

where p (respectively, $n - p$) of the subscript indices on G are 1 (2), and $G^{(n)}_{i_1 i_2 \ldots i_n}(\tilde{x},\tilde{f})$ is the corresponding nonlinear response function of an ideal Gaussian chain with the composition $\tilde{f}$ for the periodicity parameter $\tilde{x}$: the correlators $G^{(n)}_{i_1 i_2 \ldots i_n}(\tilde{x},\tilde{f})$ has to be calculated in zero-electric field for a Gaussian chain, as if it would have the composition $\tilde{f}$.

A straightforward substitution of correlators (eq 33) in eq 26 gives (Appendix E) the free energy of a copolymer melt in an electric field:

$$\Gamma_2(f,\{\vec{Q}_k\},E) = G^{(2)}_{ij}(\tilde{f},\tilde{x})\left\{\frac{\tilde{f}G^{-1}_{i1}(\tilde{f},\tilde{x})}{f} - \frac{(1-\tilde{f})G^{-1}_{i2}(\tilde{f},\tilde{x})}{(1-f)}\right\} \times \left\{\frac{\tilde{f}G^{-1}_{j1}(\tilde{f},\tilde{x})}{f} - \frac{(1-\tilde{f})G^{-1}_{j2}(\tilde{f},\tilde{x})}{(1-f)}\right\}$$

$$\Gamma_3(f,\{\vec{Q}_k\},E) = -G^{(3)}_{ijk}(\tilde{f},\tilde{x})\left\{\frac{\tilde{f}G^{-1}_{i1}(\tilde{f},\tilde{x})}{f} - \frac{(1-\tilde{f})G^{-1}_{i2}(\tilde{f},\tilde{x})}{(1-f)}\right\} \times \left\{\frac{\tilde{f}G^{-1}_{j1}(\tilde{f},\tilde{x})}{f} - \frac{(1-\tilde{f})G^{-1}_{j2}(\tilde{f},\tilde{x})}{(1-f)}\right\} \times \left\{\frac{\tilde{f}G^{-1}_{k1}(\tilde{f},\tilde{x})}{f} - \frac{(1-\tilde{f})G^{-1}_{k2}(\tilde{f},\tilde{x})}{(1-f)}\right\} \tag{34}$$

$$\Gamma_4(f,\{\vec{Q}_k\},E) = \gamma_{ijkl}(\tilde{f},\tilde{x},h_1,h_2)\left\{\frac{\tilde{f}G^{-1}_{i1}(\tilde{f},\tilde{x})}{f} - \frac{(1-\tilde{f})G^{-1}_{i2}(\tilde{f},\tilde{x})}{(1-f)}\right\} \times \left\{\frac{\tilde{f}G^{-1}_{j1}(\tilde{f},\tilde{x})}{f} - \frac{(1-\tilde{f})G^{-1}_{j2}(\tilde{f},\tilde{x})}{(1-f)}\right\} \times \left\{\frac{\tilde{f}G^{-1}_{k1}(\tilde{f},\tilde{x})}{f} - \frac{(1-\tilde{f})G^{-1}_{k2}(\tilde{f},\tilde{x})}{(1-f)}\right\} \times \left\{\frac{\tilde{f}G^{-1}_{l1}(\tilde{f},\tilde{x})}{f} - \frac{(1-\tilde{f})G^{-1}_{l2}(\tilde{f},\tilde{x})}{(1-f)}\right\}$$

where G^{-1}_{ij} is the (ij) component of the matrix inverse of the matrix $G^{(2)}_{ij}, G^{-1}_{ij}(0) = N^{-1}$:

$$\gamma_{ijkl}(\tilde{f},\tilde{x},h_1,h_2) = G^{(3)}_{ijm}(h_1)G^{-1}_{mn}(h_1\tilde{x})G^{(3)}_{nkl}(h_1) + G^{(3)}_{ilm}(h_2)G^{-1}_{mn}(h_1\tilde{x})G^{(3)}_{nkj}(h_2) + G^{(3)}_{ikm}(h_2)G^{-1}_{mn}(h_1\tilde{x})G^{(3)}_{njl}(h_2) - -G^{(4)}_{ijkl}(\tilde{f},\tilde{x},h_1,h_2)$$

and

$$\tilde{x}(\vec{Q}_1 + \vec{Q}_2) = h_1\tilde{x}(Q_1)$$

$$\tilde{x}(\vec{Q}_1 + \vec{Q}_4) = h_2\tilde{x}(Q_1)$$

In writing the correlation functions G, we have introduced notations similar to those used for coefficients Γ_3 and Γ_4 in ref 4. For instance, $G^{(3)}_{ilm}(\vec{Q}^*_1,\vec{Q}^*_2,\vec{Q}^*_3)$ correlator is denoted by $G^{(3)}_{ilm}(h)$, where for the critical wave vectors $\vec{Q}^*_1$, $\vec{Q}^*_2$ one has $\tilde{x}(\vec{Q}^*_1 + \vec{Q}^*_2) = \tilde{x}(\vec{Q}^*_3) = h\tilde{x}(\vec{Q}^*_1)$. All the correlators $G^{(n)}$ are calculated for Gaussian ideal copolymer chains.[4] Expansion 25 suggests[11] that the microphase separation in an applied electric field also occurs as a second or weak first-order transition.

To summarize, we developed the random phase approximation by calculation of response functions at the spinodal point. Our results, based on the statistics of quasi-noninteracting chains in a homogeneous electric field, are correct only near the spinodal point (as any Landau theory of weak first-order transitions).

The influence of an electric field on the microphase separation is seen to result mainly in rescaling of the periodicity parameter and renormalization of the bare composition

$$x \to \tilde{x} \qquad f \to \tilde{f}$$

The effective composition $\tilde{f}$ depends upon the applied electric field and wave vectors. It has to be considered as an additional degree of freedom besides with the order parameter ψ and the periodicity x^* of arising structure. (The physical meaning of the effective composition $\tilde{f}$ and periodicity parameters and $\tilde{x}$ are discussed in sections 5 and 7.) The normalizing factor

$$\left(\frac{f}{\tilde{f}}\right)^p\left(\frac{1-f}{1-\tilde{f}}\right)^{n-p}$$

which figures in mapping (eq 33) is an artifact of the order parameter definition.

7. Radiation Scattering by Liquid Copolymers in an Electric Field. Four Universal Classes

Radiation scattering experiments could provide an attractive method for studying the influence of an electric field on the microphase separation. In the present section, we discuss scattering by the disordered phase with emphasis on the role of the electric field. We show that copolymer melts reveal four different universal type of behavior in an applied field.

Scattering Function. The scattering intensity for a disordered melt of block copolymers is proportional to the correlation function $S(\vec{Q})$ of composition fluctuations, given by

$$S(\vec{Q}) = N/[\Gamma_2(E,f) - 2\chi N] \qquad (35)$$

Here, the vertex Γ_2 in an electric field defined by eqs 26 and 34 (see Appendix E) is

$$\Gamma_2(f,E,Q) = G^{(2)}_{ij}(\tilde{x},\tilde{f})\left(\frac{\tilde{f}G^{-1}_{i1}(\tilde{x},\tilde{f})}{f} - \frac{(1-\tilde{f})G^{-1}_{i2}(\tilde{x},\tilde{f})}{1-f}\right)\times \left(\frac{\tilde{f}G^{-1}_{j1}(\tilde{x},\tilde{f})}{f} - \frac{(1-\tilde{f})G^{-1}_{j2}(\tilde{x},\tilde{f})}{1-f}\right)$$

where $G^{(2)}_{ij}(f,x)$, $G^{-1}_{ij}(f,x)$ are response functions of an ideal Gaussian copolymer chain defined and calculated in ref 4 for the periodicity parameter, x, and the composition, f. The effective periodicity parameter, $\tilde{x}$, and effective composition, $\tilde{f}$, introduced in eq 32, are

$$\tilde{x} = x^{(A)}f + x^{(B)}(1-f)$$

$$\tilde{f} = fx^{(A)}/\tilde{x} \qquad (36)$$

Note, that $x^{(A)}$ and $x^{(B)}$ are complex functions (eq 21) of the electric field intensity and of the anisotropic parts of A and B link polarizabilities.

Periodicity Parameter. The periodicity parameter x naturally appeared in the Leibler theory.[4] It shows that the only characteristic size near microphase separation is a gyration radius. The fact that in an electric field all correlators depend upon the periodicity parameter $\tilde{x}$ shows that the size of the gyration ellipsoid remains the only characteristic size in an electric field as well. Indeed, $\tilde{x}$, defined by eq 36, can be rewritten as

$$\tilde{x} = (\vec{Q}\vec{R})^2$$

where $\vec{R}$ is the end-to-end vector (eq 18) of a quasi-noninteracting copolymer chain in the electric field.

Renormalization of Composition. The new parameter $\tilde{f}(E,\vec{Q})$, introduced above, has to be be treated as a new "composition" of the chain in an electric field. In the absence of an electric field, $\tilde{f}(E,\vec{Q})$ coincides with f.

The electric field changes the persistence lengths of A and B units differently. The stiffness of A and B blocks along and perpendicular to the field are also different. As a result, the composition of the diblock measured in numbers of statistical segments of blocks is ambiguous: the entropy of ordered chains becomes a function of some very refined effective composition, $\tilde{f}$ (see section 5). The theoretical realization of that simple physical picture, unfortunately, takes an accurate construction of map (eq 33) and the self-consistent approach (section 3) for an electric field. From eq 36 one gets

$$\frac{\tilde{f}}{1-\tilde{f}} = \frac{fx^{(A)}}{(1-f)x^{(B)}}$$

The effective composition, which appears naturally in the theory, turns out to be the composition (eq 24), namely, the composition measured in numbers of statistical segments along the vector $\vec{Q}$.

Spinodal Line and Critical Fluctuations in an Electric Field. The scattering function (eq 35) shows (Appendix F) that, for large and for small wave vectors, respectively, the intensity $S(\vec{Q})$ tends to zero like:

$$S(\vec{Q}) = \frac{2}{(\vec{Q}\vec{R})^2}\left(\frac{\tilde{f}}{f^2} + \frac{(1-\tilde{f})}{(1-f)^2}\right)^{-1}$$

$$S(\vec{Q}) = \frac{2}{3}(\vec{Q}\vec{R})^2f^2(1-f)^2$$

For small Q the light-scattering functions reveal incred-

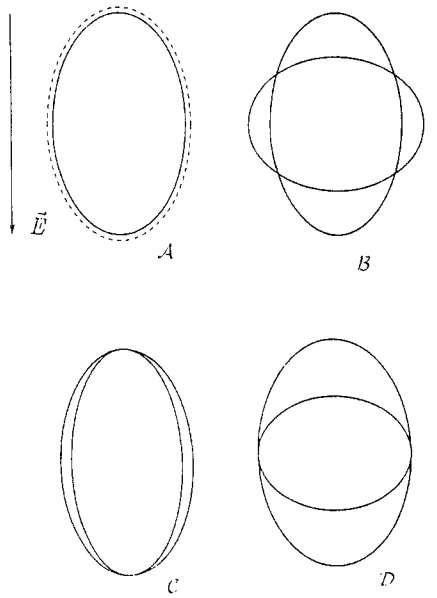

Figure 6. Four topologically distinct types with two axial ellipsoids intersecting. They correspond to four universal classes, A, B, C, and D, of a copolymer melt behavior under a field which orients the repeat units of chains.

ibly complicated dependence upon the direction of $\vec{Q}$ (recall that $\tilde{f}$ is also a function of Q).

These asymptotics require that for intermediate wave vectors, the scattering function has a peak (a maximum). The position $\tilde{x}^*$, f^* of the peak (Figures 9 and 10) does not depend on the monomer–monomer interaction, χ. In fact, expression 35 has a maximum for $\tilde{x}^*, f^*$ for which the χ-independent function $\Gamma_2(f,\tilde{x}^*,f^*)$ has a minimum. It is very important to stress that $\tilde{x}^*$ and f^* depend neither on the Flory–Huggins parameter χ, nor upon an applied electric field, E, nor upon the degree of polymerization, N. They are functions only of the "bare" composition, f.

The values $\tilde{x}^*$ and f^* define the critical wave vectors Q^*: at the spinodal point, $(\chi N)_c$, the fluctuations with this wave vector diverge. The critical wave vectors are given by eq 37:

$$f^*\tilde{x}^* = (Q_1^*R_1^{(A)})^2 + (Q_p^*R_p^{(A)})^2$$
$$(1-f^*)\tilde{x}^* = (Q_1^*R_1^{(B)})^2 + (Q_p^*R_p^{(B)})^2 \qquad (37)$$

These equations describe two ellipsoids in Q-space. The physics of microphase separation depends on the way these ellipsoids intersection (Figure 6). Four topologically distinct situations are possible.

Class $\mathcal{A}$. Critical Ellipsoid. Degeneration-in-Electric Field. Let us consider the case, when the anisotropic parts of the A and B units, $\nu^{(A)}$ and $\nu^{(B)}$, are equal. (Since the effective Flory-Huggins repulsion appears, generally speaking, as a result of a difference of polarizability properties of the A and B links, the isotropic parts, $\alpha^{(A)}$ and $\alpha^{(B)}$, of their polarizabilities have to be different.) In such a case, A and B blocks are deformed by the field in the same way: $S^{(B)} = S^{(A)} = S(E)$.

From eq 36, it follows that the effective composition, $\tilde{f}$, is identically equal to f. The scattering function read formally as in ref 4:

$$\Gamma_2(f,\tilde{x}) = G_{ij}^{(2)}(f,\tilde{x})(G_{i1}^{-1}(f,\tilde{x}) - G_{i2}^{-1}(f,\tilde{x}))(G_{j1}^{-1}(f,\tilde{x}) - G_{j2}^{-1}(f,\tilde{x}))$$

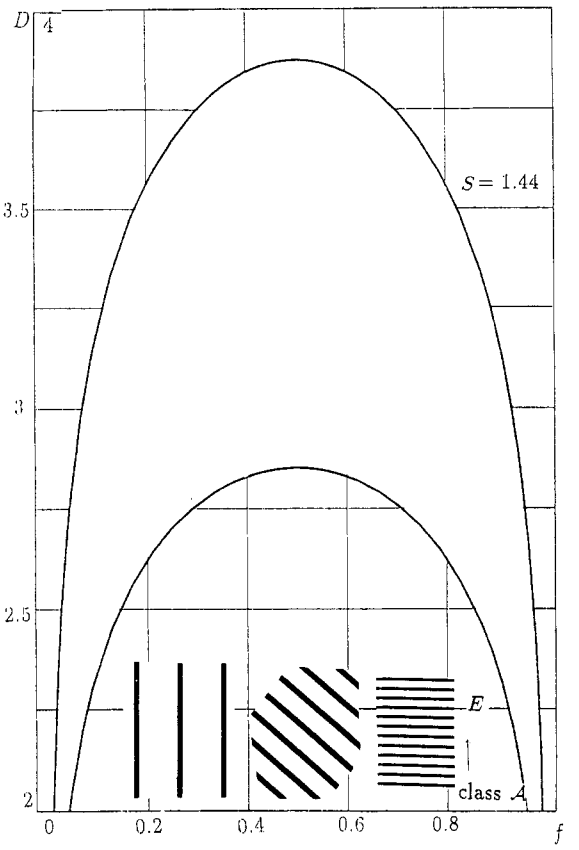

Figure 7. The periodicity, D, of the structure vs f for a copolymer melt of class A (in units of gyration radius, R); S is 1.44. D is nonfixed and depends on the structure orientation with respect to the field as well as on the field intensity, E.

The critical value of the parameter periodicity, $\tilde{x}^*$, is given by the minimum of $\Gamma_2(f,\tilde{x})$ over $\tilde{x}$. It depends only upon composition f as in the absence of an electric field. The spinodal line

$$(\chi N)_c = \Gamma_2(f,x^*)$$

determines the limit of homogeneous copolymer melts metastability in an electric field. The value of the spinodal line $(\chi N)_c$ at which the instability would occurs depends solely upon the composition f and coincides with the spinodal point for the very same melt in the absence of an electric field. Thus, for the copolymer of class $\mathcal{A}$, the spinodal point will not be shifted by an electric field.

Equations 37 are degenerated in an equation of one critical ellipsoid:

$$x^* = (Q_1^*R_1)^2 + (Q_p^*R_p)^2 \qquad (38)$$

All the fluctuations with wave vectors belonging to this ellipsoid diverge at the spinodal point, $(\chi N)_c$.

The value of the critical wave vector depends, of course, upon the electric field intensity, E, as well as upon the wave vector orientation with respect to the applied field. The amplitudes of the critical wave vectors along and perpendicular to the electric field are limited as follows

$$\frac{x^*}{R_p^2} < (Q^*)^2 < \frac{x^*}{R_1^2}$$

It implies that the periodicity of the pattern ranges between two limit values and, strictly speaking, is nonfixed (Figure 7). The case[4] of zero electric field is a special case of class $\mathcal{A}$ considered above: it corresponds to $S^{(B)}$, $S^{(A)} = 1$, for which eq 38 describes the critical sphere (eq 29). The dependence of the periodicity

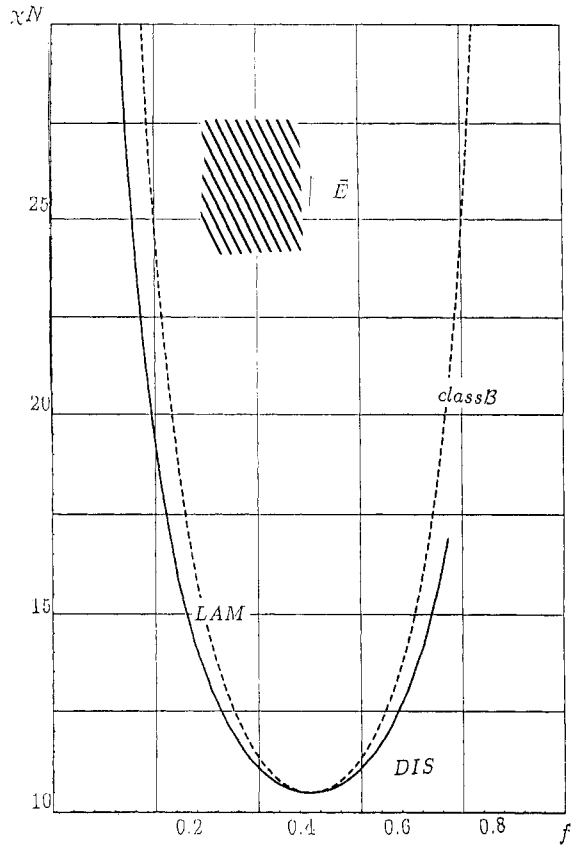

Figure 8. The spinodal point vs f for a copolymer melt of class B. It does not depend on the electric field intensity and is always less than the spinodal (dashed line) for zero electric field. The phase diagram for a diblock copolymer melt of class $\mathscr{B}$. It presents the stability regions of a one-dimensional lamellar phase in the plane with coordinates f and χN. At the spinodal point a second-order transition occurs from disordered to a lamellar phase for any composition f. The lamellar phase is tilted with respect to the field.

parameter, $\tilde{x}^*$, and the spinodal point, $(\chi N)_c$, vs f are the same as those illustrated in Figures 2 and 4 for a zero-electric field.[4]

Class $\mathscr{B}$. Two Critical Rings. In the general case, the anisotropic parts of links polarizability tensors are different and equations 37 describe two ellipsoids. If the following unequalities hold

$$\begin{cases} \dfrac{(R_l^{(A)})^2}{(R_l^{(B)})^2} < \dfrac{f^*}{1-f^*} > \dfrac{(R_p^{(A)})^2}{(R_p^{(B)})^2} \\ \cup \\ \dfrac{(R_l^{(A)})^2}{(R_l^{(B)})^2} > \dfrac{f^*}{1-f^*} < \dfrac{(R_p^{(A)})^2}{(R_p^{(B)})^2} \end{cases}$$

the ellipsoids intersect each other along two rings. This condition can be treated as follows: the effective composition, f^*, which provides the absolute minimum of the free energy, is less (larger) than the composition associated with Kuhn lengths measured along the electric field, but f^* is larger (less) than that measured in Kuhn lengths perpendicular to the electric field. A copolymer can belong to class $\mathscr{B}$ only if the composition, f, ranges between 0.331 and 0.669.

The spinodal point is

$$(\chi N)_c = \Gamma_2(f,\tilde{x}^*,f^*) \tag{39}$$

where $\tilde{x}^*$ and f^* depend in turn solely on the composition, f. Thus, the spinodal point also depends solely upon the composition, f, and is shown in Figure 8.

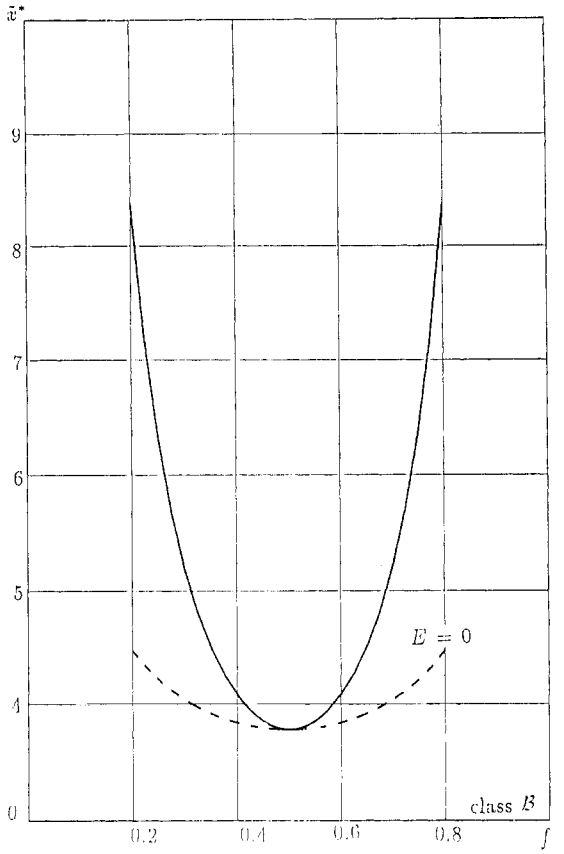

Figure 9. The equilibrium periodicity parameter, $\tilde{x}^*$, vs f for a copolymer melt of class $\mathscr{B}$ (in units of gyration radius, R). $\tilde{x}^*$ is independent of the electric field intensity. For a given composition, f, $\tilde{x}^*$ is always larger than the periodicity parameter, x^* (dashed line) for zero electric field.[4]

The fluctuations with wave vectors Q^* belonging to the rings of the ellipsoids intersection diverge at the spinodal point, $(\chi N)_c$. The critical wave vectors are complicated function of composition f. In a matrix form the solution of equations 37 reads

$$\begin{vmatrix} Q_l^{*2} \\ Q_p^{*2} \end{vmatrix} = \begin{vmatrix} (R_l^{(A)})^2 & (R_p^{(A)})^2 \\ (R_l^{(B)})^2 & (R_p^{(B)})^2 \end{vmatrix}^{-1} \begin{vmatrix} \dfrac{\tilde{x}^* f^*}{f} \\ \dfrac{\tilde{x}^*(1-f^*)}{1-f} \end{vmatrix}$$

The effective composition, f^*, and periodicity parameter, $\tilde{x}^*$, were introduced by equation 37 and are shown in Figures 9 and 10. The square of tangence between the critical wave vector and the applied electric field is

$$\frac{(R_p^{(B)})^2 f^* - (R_p^{(A)})^2(1-f^*)}{(R_l^{(A)})^2(1-f^*) - (R_p^{(B)})^2 f^*} = \frac{1}{2}\frac{(3-S^{(B)})\mathscr{A}(f) - (3-S^{(A)})}{S^{(A)} - S^{(B)}\mathscr{A}(f)} \tag{40}$$

where we introduced the function

$$\mathscr{A}(f) = \frac{(1-f)f^*}{f(1-f^*)}$$

The angle depends neither upon the degree of polymerization, N, nor on the Flory–Huggins interaction parameter, χ. (The function $\mathscr{A}$ is shown in Figure 13.)

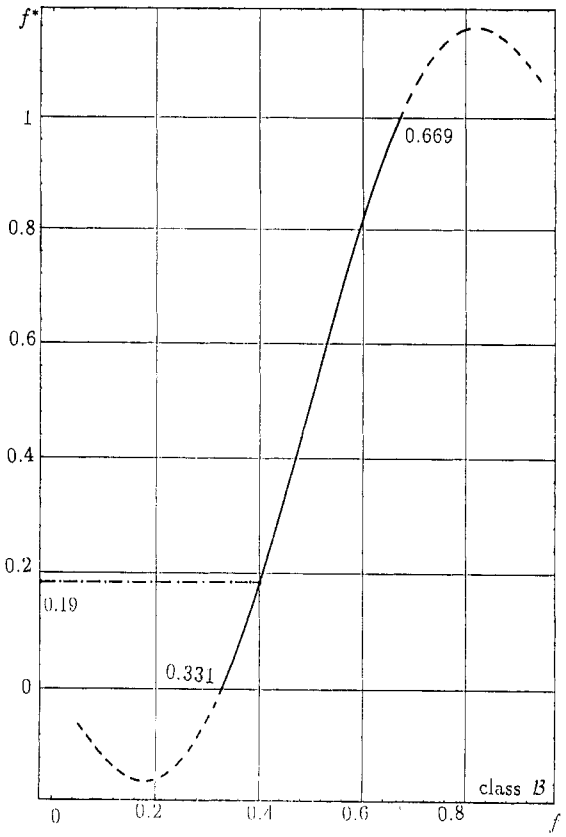

Figure 10. The equilibrium effective composition, f^*, vs the composition, f, for a copolymer melt of class $\mathscr{B}$. f^* is an universal function solely of f: it does not depend on the electric field and the Flory–Huggins interaction parameter, χ. For instance, for $f = 0.4$, f^* is 0.19.

Class $\mathscr{C}$. Two Critical Points. When

$$\begin{cases} \dfrac{f^*}{1-f^*} < \dfrac{(R_1^{(A)})^2}{(R_1^{(B)})^2} < \dfrac{(R_p^{(A)})^2}{(R_p^{(B)})^2} \\ \cup \\ \dfrac{f^*}{1-f^*} < \dfrac{(R_1^{(A)})^2}{(R_1^{(B)})^2} < \dfrac{(R_p^{(A)})^2}{(R_p^{(B)})^2} \end{cases}$$

ellipsoids do not intersect each other at all. At

$$\chi N = \Gamma_2(f,\tilde{x}^*,f^*)$$

the light-scattering function reveals two diffusive points in Q-space in the vicinity of ellipsoids polices. That is, no real wave vectors correspond to values f^* and $\tilde{x}^*$ for which the function $\Gamma_2(f,\tilde{x}^*,f^*)$ has the absolute minimum. The real spinodal line corresponds to some smaller values, $(\chi N)_c$, which could be defined as a possible minimum value:

$$(\chi N)_c(E) = \Gamma_2(f,x_*^*(E),f_*^*(E))$$

such that for

$$\tilde{x} = x_*^*(E) \qquad \tilde{f} = f_*^*(E)$$

system 37 would have at least one real solution in Q-space. This solution arises when ellipsoids touch each other in the pole points placed along an electric field.

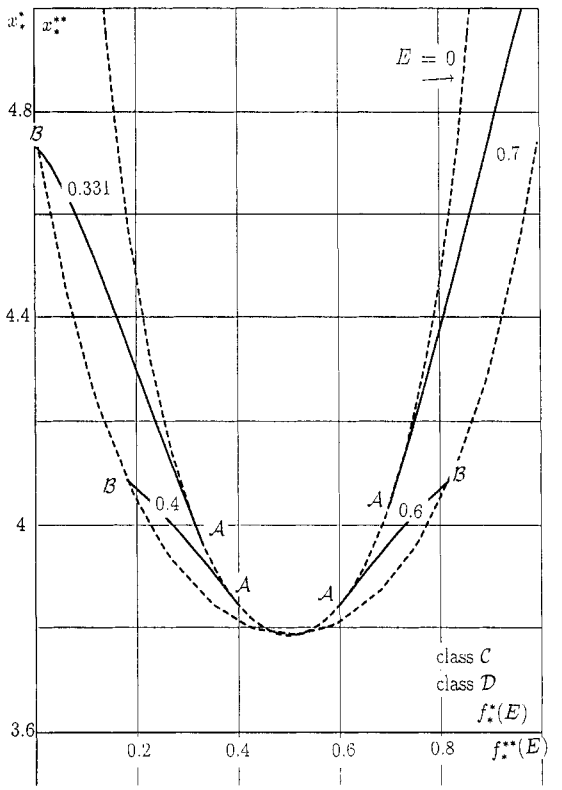

Figure 11. The equilibrium periodicity parameter for classes $\mathscr{C}(\mathscr{D})$, x_*^*, (x_*^{**}), vs f_*^* (f_*^{**}) for $f = 0.331$, 0.4, 0.6, and 0.7. For a given composition, f, x_*^* (x_*^{**}) is always larger than the periodicity parameter, x^*, for zero electric field[4] but is less than the periodicity parameter, $\tilde{x}^*$, for class B. Points $\mathscr{A}$ correspond to the zero electric field case: f_*^* $(f_*^{**}) = f$ and x_*^* $(x_*^{**}) = x^*$. Points $\mathscr{B}$ correspond to class B: f_*^* $(f_*^{**}) = \tilde{f}^*(f)$ and x_*^* $(x_*^{**}) = \tilde{x}^*(f)$.

From equations 37 one finds that the effective composition corresponding to this "touch", f_*^*, is

$$\frac{f_*^*}{1-f_*^*} = \frac{fS^{(A)}(E)}{(1-f)S^{(B)}(E)} = \frac{(R_1^{(A)})^2}{(R_1^{(B)})^2}$$

This implies that the effective composition f_*^* is measured in numbers of Kuhn lengths of A and B blocks along the electric field (see section 4). The equilibrium periodicity parameter, $x_*^*(E)$, provides a minimum of $\Gamma_2(f,\tilde{x},f_*^*)$ for fixed f and f_*^*. The dependence $x_*^*(E)$ vs $f_*^*(E)$ is given in Figure 11. In an applied electric field for a copolymer melt of class C, the periodicity parameter x_*^* is larger than that for zero electric field (points A in Figure 11) and less than that for class $\mathscr{B}$ (points $\mathscr{B}$ in Figure 11).

The spinodal point $\Gamma_2(f,x_*^*,f_*^*)$ depends on the applied electric field, E, and on the composition, f. For several different compositions the dependence of the spinodal point on the intensity of the applied field (vs $F_*^*(E)$) is shown in Figure 12.

The critical wave vector is oriented along the electric field ($Q_p^* = 0$) and

$$(Q_1^*)^2 = \frac{x_*^*(E)}{(R_1^{(A)})^2 + (R_1^{(B)})^2} \tag{41}$$

Its absolute value depends on f and E.

Class $\mathscr{D}$. One Critical Ring. The third type of copolymer melts in an electric field corresponds to the case

$$\begin{cases} \dfrac{f^*}{1-f^*} < \dfrac{(R_p^{(A)})^2}{(R_p^{(B)})^2} < \dfrac{(R_1^{(A)})^2}{(R_1^{(B)})^2} \\ \cup \\ \dfrac{f^*}{1-f^*} < \dfrac{(R_p^{(A)})^2}{(R_p^{(B)})^2} < \dfrac{(R_1^{(A)})^2}{(R_1^{(B)})^2} \end{cases}$$

Ellipsoids also do not intersect each other: χN equals the absolute minimum of the $\Gamma_2(f,\tilde{x}^*,f^*)$. System 37 does not have any solutions for real wave vectors. That is, no real wave vectors correspond to values f^*, and $\tilde{x}^*$ for which the function $\Gamma_2(f,\tilde{x}^*,f^*)$ has the absolute minimum. The real spinodal line corresponds to some smaller values, $(\chi N)_c$, which could be defined as a possible minimum value, $\Gamma_2(f,x_*^{**}(E),f_*^{**}(E))$, such that for

$$\tilde{x} = x_*^{**}(E) \qquad \tilde{f} = f_*^{**}(f)$$

equation 37 would define at least a one real critical wave vector. It happens when ellipsoids touch each other along their diameter perpendicularly to the electric field. The effective composition corresponding to this "touch", f_*^{**}, is

$$\frac{f_*^{**}}{1-f_*^{**}} = \frac{(3-S^{(A)})}{(3-S^{(B)})}\frac{f}{1-f} = \frac{(R_p^{(A)})^2}{(R_p^{(B)})^2}$$

For copolymer melts of class $\mathcal{D}$, the equilibrium value of the effective composition, f_*^{**}, is seen to be defined in Kuhn lengths, which are measured perpendicularly to the field. The spinodal point

$$(\chi N)_c = \Gamma_2(f,f_*^{**})$$

is a function of an applied electric field and the composition, f (Figure 12).

The periodicity parameter, $x_*^{**}(E)$, is defined as a minimum of $\Gamma_2(f,\tilde{x},f_*^{**}(E))$ over $\tilde{x}$ for fixed f and $f_*^{**}(E)$. The dependence of the periodicity parameter, x_*^{**}, on the electric field intensity [strictly speaking, on $f_*^{**}(E)$] is given in Figure 11. Critical wave vector are directed strictly perpendicular to the electric field:

$$(Q_p^*)^2 = \frac{x_*^{**}(E)}{(R_p^{(A)})^2 + (R_p^{(B)})^2} \tag{42}$$

The length of the critical wave vector depends upon the composition, f, and the intensity, E.

We renumerated and described above four classes of copolymer melts in an electric field. These classes are rather universal: neither the Flory–Huggins parameter, χ, nor the degree of polymerization, N, will change the class of universality of a copolymer melt.

How To Define What Class a Copolymer Melt Belongs to? Phase Diagram Of Universal Classes. The microphase separation occurs as a competition between the Flory–Huggins repulsion energy and the entropy of ordering. The latter depends on the effective composition, $\tilde{f}$, rather then on the bare composition, f. This effective composition, $\tilde{f}$, has to be treated as an additional degree of freedom (besides the periodicity x). The minimization of the free energy over $\tilde{f}$ gives its equilibrium values: f, f^*, f_*^*, and f_*^{**} for the universal classes $\mathcal{A}$, $\mathcal{B}$, $\mathcal{C}$, and $\mathcal{D}$, respectively. The effective composition for class $\mathcal{A}$ is identically equals to the "bare" compositions, f. The effective composition, f^*, of class

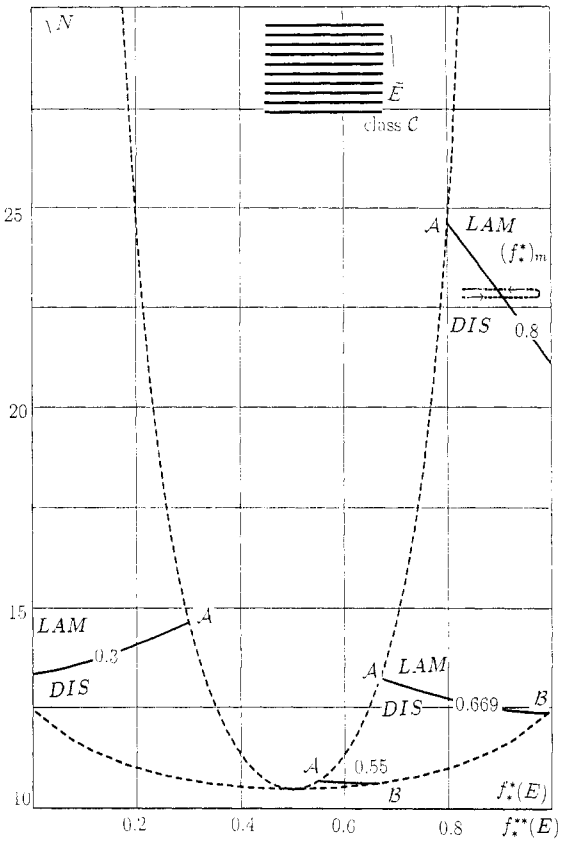

Figure 12. The spinodal point for a copolymer melt of classes $\mathcal{C}$ ($\mathcal{D}$) vs f_*^* (f_*^{**}) for $f = 0.3$, 0.55, 0.669, and 0.8. The upper dashed line is the spinodal[4] for zero electric field case. The phase diagram for a diblock copolymer melt of class C. At the spinodal point, a second-order transition occurs from a disordered melt to a lamellar phase. This lamellar phase is oriented perpendicular to the field. For the diblock melt with $f = 0.8$, arrows show a reentrant phase behavior induced by the applied field (see section 10).

$\mathcal{B}$ corresponds to the absolute minimum of Γ_2 vertex and is some universal function of the composition, f: it depends neither upon the electric field, nor upon the degree of polymerization, nor upon the interaction parameter, χ. The equilibrium effective compositions for classes $\mathcal{C}$ and $\mathcal{D}$, f_*^* and f_*^{**}, turned out to be associated with compositions measured in Kuhn lengths along and perpendicularly to the applied field. Relations between the four characteristics of a copolymer chain, f, f^*, f_*^*, and f_*^{**}, lead to a division of copolymer melts into four classes:

$\mathcal{A}$: $f^* = f_*^* = f_*^{**}$

$\mathcal{B}$: $f_*^* > f^* > f_*^{**}$ ($f_*^* < f^* < f_*^{**}$)

$\mathcal{C}$: $f^* > f_*^* > f_*^{**}$ ($f^* < f_*^* < f_*^{**}$)

$\mathcal{D}$: $f^* > f_*^{**} > f_*^*$ ($f^* < f_*^{**} < f_*^*$)

It is convenient to present these classes and transitions between them in a universal class diagram. Since f^* is a function only of the composition f, the function

$$\mathcal{A}(f) = \frac{f^*(1-f)}{f(1-f^*)} \tag{43}$$

also depends solely upon the composition f. This dependence is shown in Figure 13. The inversion of the composition f, $f \leftrightarrow 1-f$ results in the inversion of $\mathcal{G}$, $\mathcal{S}$

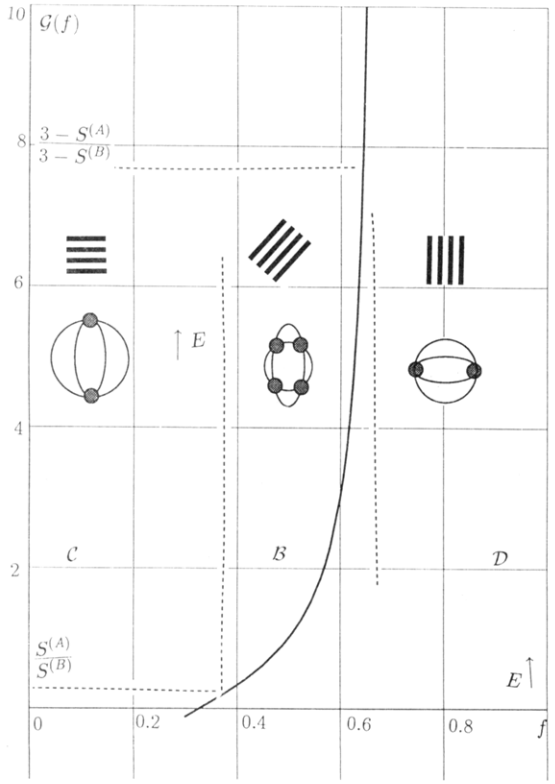

Figure 13. The diagram of universal classes for the diblock architecture. The universal function, $\mathcal{G}$, depends solely on the composition, f. It equals zero and infinity at $f = 0.331$ and 0.669, respectively.

$\leftrightarrow \mathcal{G}^{-1}$. For the symmetric copolymers, $\mathcal{G}$ equals 1. Two compositions for which the function $\mathcal{G}$ is equal to

$$\frac{3 - S^{(A)}}{3 - S^{(B)}} \qquad \frac{S^{(A)}}{S^{(B)}}$$

divide all the composition region into three classes, $\mathcal{B}$, $\mathcal{C}$, and $\mathcal{D}$, as it is shown in Figure 13. The point $\mathcal{O}$ corresponds to class $\mathcal{A}$. On decreasing the applied electric field, the composition region of class $\mathcal{B}$ virtually disappears, while classes $\mathcal{C}$ and $\mathcal{D}$ give the microphase separation picture[4] of Leibler. For experimentally available electric fields the composition region of class $\mathcal{B}$ is very narrow (section 11).

8. Orientational Phase Transitions Induced by Field

An increase of the electric field (or f) leads to transitions between different classes. For instance, a lamellar phase oriented perpendicular to the electric field should be spontaneously transformed [by orientational phase transitions, smectic A (class $\mathcal{C}$)−smectic C (class $\mathcal{B}$)−smectic A (class $\mathcal{D}$)] into a lamellar oriented parallel to the field. A melt of class $\mathcal{A}$ always remains class $\mathcal{A}$ (isomorphic to itself).

$$\mathcal{C} \overset{f,E}{\leftrightarrow} \mathcal{B} \overset{f,E}{\leftrightarrow} \mathcal{D}$$

$$\mathcal{A} \overset{f,E}{\leftrightarrow} \mathcal{A}$$

Indeed, when, for a given composition f and electric field E,

$$f^*(f) = f_*^*(f,E)$$

two critical rings degenerate into two critical points and class $\mathcal{B}$ transforms into class $\mathcal{C}$. Only fluctuations with wave vectors directed strictly parallel to the applied field diverge. Analogously, when

$$f^*(f) = f_*^{**}(f,E)$$

two critical rings dengerate into one critical ring and class $\mathcal{B}$ transforms into class $\mathcal{D}$. Only fluctuations with wave vectors directed strictly perpendicular to the applied field diverge. Orientational phase transitions can occur only for diblocks with composition f between 0.669 and 0.331.

The transitions between classes $\mathcal{C}$, $\mathcal{B}$, and $\mathcal{D}$ are not simple reorientations of the sample, but rather real second-order phase transitions, which are liquid−crystalline in nature. Lamellar phases of classes $\mathcal{C}$ and $\mathcal{D}$ are smectic A, whereas the lamellar phase for class $\mathcal{B}$ is, in fact, smectic $\mathcal{C}$. The order parameters for transitions class $\mathcal{B} \rightarrow$ class $\mathcal{C}$ and class $\mathcal{B} \rightarrow$ class $\mathcal{D}$ are[17] a two-component vector and a scalar, respectively.

9. Stability of Ordered Phases

In this section we discuss the symmetry and the periodicity of the microdomain structure appearing just after the microphase separation transition. Each of the four classes described in section 7 has its specific picture of the microphase separation. For each of them we study the stability of various microdomain patterns and determine the conditions of their equilibria. These considerations lead us to four universal types of phase diagrams for diblock copolymer melts in an electric field.

Landau Theory of the Microphase Separation. The free-energy density functional (eqs 25 and 34) obtained in section 4 should be minimized with respect to the order parameter. Within the framework of the Landau theory the only important candidates for Fourier components of the order parameter are those with critical wave vectors $\vec{Q}^*$. The order parameter is

$$\psi(\vec{r}) = \sum_{k=1}^{n} \psi(\vec{\tilde{Q}}^*) \exp i(\vec{\tilde{Q}}^*_k \vec{r})$$

where $\vec{\tilde{Q}}^* \in \{\text{critical surface in } Q\text{-space}\}$.

Weakly ordered structures are characterized by sets of critical vectors, $\{\vec{\tilde{Q}}^*_k\}$ $(k = 1, ..., n)$, which form the so-called critical star of wave vectors, $\{\vec{\tilde{Q}}^*_k\}$. The free energy depends crucially on the set $\{\vec{\tilde{Q}}^*_k\}$. In turn, the sets of possible critical wave vectors are determined by the form of the critical surface. The latter is nondependent of χN but is different for different classes of copolymers. The parameter χN cannot result in a transition between these classes, and for each class the phase diagram, as a function of χN and f, can be constructed independently. To decide which mesophase will actually appear for a given χN, it is necessary to analyze the free energy for $\mathcal{A}$, $\mathcal{B}$, $\mathcal{C}$, and $\mathcal{D}$ classes in more detail.

Class $\mathcal{A}$. A copolymer having equal anisotropic polarizabilities of A and B units reveals some amusing symmetry properties in an electric field (section 7). The spinodal line, $(\chi N)_c$, depends only on the composition, f, and equals that[4] in the absence of electric field. The critical surface in Q-space is an ellipsoid described by equation 38.

In the free energy expansion, the negative third-order term favors the appearance of the complex ordered structures forming triangles from the critical wave vectors. The condition for three vectors on a ellipsoid

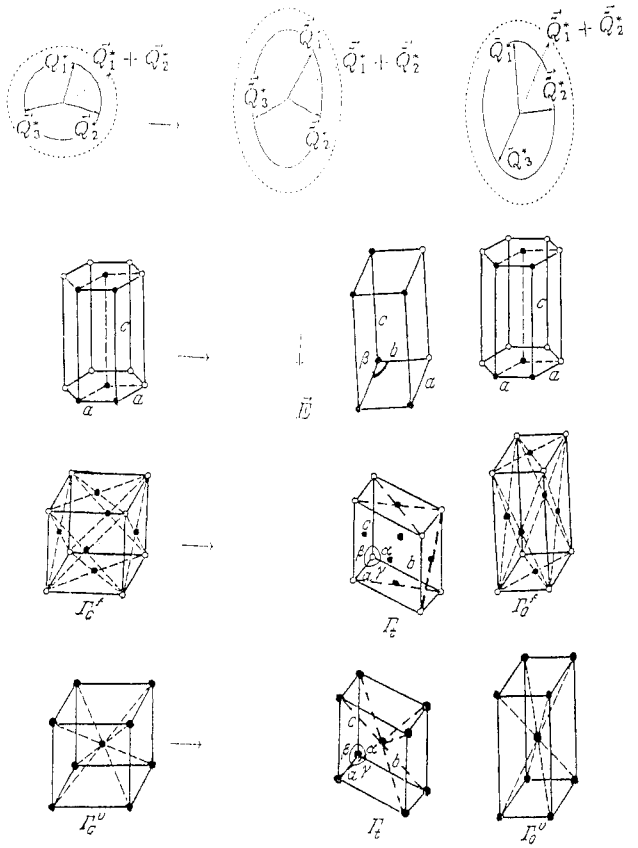

Figure 14. (top) Rescaling of space (section 2, eq 10) which maps a homopolymer chain deformed by an electric field in an ideal Gaussian chain. Rescaling of space (section 7, eq 44) which maps a copolymer of class $\mathcal{A}$ in an ideal Gaussian chain. The very same rescaling in Q-space maps the sphere (eq 29) of critical wave vectors for zero electric field[4] into the ellipsoid (eq 38) of critical wave vectors for nonzero field. (bottom) The equilibrium structures in an applied electric field. One-dimensional lamellar, two-dimensional monoclinic lattice, and three-dimensional triclinic lattices are shown in $\tilde{Q}$- and $\tilde{r}$-spaces. If the pattern is spontaneously oriented along the field, the two last structures have the symmetries of body-centered tetragonal and honeycomb (hexagonal) structures, respectively.

to make a triangle, $\tilde{\vec{Q}}_1 + \tilde{\vec{Q}}_2 + \tilde{\vec{Q}}_3 = 0$, is very difficult to formulate mathematically. Needless to say, a straightforward calculation of the free energy for different sets of critical wave vectors on the critical ellipsoid would require rather tedious calculations of $\Gamma_3(\tilde{\vec{Q}}_1,\tilde{\vec{Q}}_2,\tilde{\vec{Q}}_3)$ and $\Gamma_4(\tilde{\vec{Q}}_1,\tilde{\vec{Q}}_2,\tilde{\vec{Q}}_3,\tilde{\vec{Q}}_4)$. We will escape all the direct calculations by using the space rescaling [see sections 2 (eq 10) and 6 (eq 32)].

Rescaling of Space or Affine Transformation. It is very fruitful to note that rescaling (eq 10) of the real $\vec{r}$-space transforms a polymer homogeneously deformed by an electric field into a Gaussian chain (Figure 14). Respectively, in reciprocal Q-space, the same rescaling

$$Q_l^2 \to Q_l^2/S$$

$$Q_p^2 \to Q_p^2 2/(3 - S) \qquad (44)$$

transforms the critical ellipsoid into the critical sphere. To put it another way, if a vector $\tilde{\vec{Q}}^*$ belongs to the critical ellipsoid (eq 38)

$$x(\tilde{\vec{Q}}^*) = \tilde{x}^*$$

its image, Q^*, given by eq 44 lies on the critical sphere (eq 29), that is,

$$x(\vec{Q}^*) = x^*$$

In the same way, any set, $\{\vec{Q}^*\}$, of critical wave vectors (associated with a specific structure in zero electric field) on the critical sphere corresponds to one and only one set, $\{\tilde{\vec{Q}}^*\}$, of critical wave vectors on the ellipsoid. In an applied electric field (the case of an ellipsoid) one has an infinite number of essentially different sets even for a given Bravais lattice in zero field (case of a sphere). For example, the simplest lamellar phases described by a single wave vector, $\vec{Q}^*_{l1}$, on the critical ellipsoid are different: the lamellar phase periodicity depends upon the direction of the symmetry breaking with respect to the direction of the electric field (see Figures 7 and 14).

We will prove below that in an electric field the free energies of all structures, $\{\tilde{\vec{Q}}^*\}$, coming from the same Bravais lattice, $\{\vec{Q}^*\}$, on the critical sphere via mapping (eq 44) are equal to each other and to the free energy of the structure $\{\vec{Q}^*\}$ in zero field.

Firstly, we note that if $\vec{Q}_1 + \vec{Q}_2 + \vec{Q}_3 = 0$ (or $\vec{Q}_1 + \vec{Q}_2 + \vec{Q}_3 + \vec{Q}_4 = 0$) for wave vectors on the critical sphere, the same equations hold for their images, $\tilde{\vec{Q}}_k$, on the critical ellipsoid. The latter follows from the fact that a linear transformation always maps the zero wave vector into itself.

In an electric field, $\Gamma_3(\tilde{\vec{Q}}_1,\tilde{\vec{Q}}_2,\tilde{\vec{Q}}_3)$ vanishes unless $\tilde{\vec{Q}}_1 + \tilde{\vec{Q}}_2 + \tilde{\vec{Q}}_3 = 0$. In zero field, all nonvanishing $\Gamma_3(\vec{Q}_1,\vec{Q}_2,\vec{Q}_3)$ functions are equal since $|\vec{Q}_1| = |\vec{Q}_2| = |\vec{Q}_3| = Q^*$. In an applied field, the critical wave vectors $\tilde{\vec{Q}}_1^*$, $\tilde{\vec{Q}}_2^*$, $\tilde{\vec{Q}}_3^*$ have different lengths, but they enter the free energy only in the combination $\tilde{x}(\tilde{\vec{Q}})$. Since these vectors are critical, $\tilde{x}(\tilde{\vec{Q}}^*) = x^*$. That is, Γ_3 does not depend on the actual set of vectors $(\tilde{\vec{Q}}_1^*, \tilde{\vec{Q}}_2^*, \tilde{\vec{Q}}_3^*)$ but only on x^*. As a result, one concludes that all nonvanishing $\Gamma_3(\tilde{\vec{Q}}_1,\tilde{\vec{Q}}_2,\tilde{\vec{Q}}_3)$ are equal to each other in spite of the fact that different sets of $\tilde{\vec{Q}}_1^*$, $\tilde{\vec{Q}}_2^*$, $\tilde{\vec{Q}}_3^*$ describe quite different patterns. This function will be denoted by $\Gamma_3(f,x^*)$ and coincides with $\Gamma_3(f,x^*)$ calculated in ref 4 for the critical sphere case:

$$\Gamma_3(f,\{\tilde{\vec{Q}}^*\},E) = \Gamma_3(f,x^*) \qquad (45)$$

An analysis of Γ_4 is more complicated. Indeed, the fourth-order vertex, $\Gamma_4(\tilde{\vec{Q}}_1^*,\tilde{\vec{Q}}_2^*,\tilde{\vec{Q}}_3^*,\tilde{\vec{Q}}_4^*)$, depends not only upon $x(\tilde{\vec{Q}}_1^*) = x(\tilde{\vec{Q}}_2^*) = x(\tilde{\vec{Q}}_3^*) = x(\tilde{\vec{Q}}_4^*) = x^*$ but also upon intermediate wave vectors $\tilde{\vec{Q}}_1^* + \tilde{\vec{Q}}_2^*$ and $\tilde{\vec{Q}}_1^* + \tilde{\vec{Q}}_4^*$. The last two vectors do not belong to the critical ellipsoid (see Figure 14). It is convenient to adopt the notations

$$\tilde{x}(\tilde{\vec{Q}}_1^* + \tilde{\vec{Q}}_2^*) = h_1 x^*$$

$$\tilde{x}(\tilde{\vec{Q}}_1^* + \tilde{\vec{Q}}_4^*) = h_2 x^* \qquad (46)$$

All nonvanishing Γ_4 vertices in an applied field depend only upon x^*, h_1, h_2, and composition f.

The vector $\tilde{\vec{Q}}_1^* + \tilde{\vec{Q}}_2^*$ ($\tilde{\vec{Q}}_1^* + \tilde{\vec{Q}}_4^*$) lies on an ellipsoid h_1 (h_2) times larger than the critical ellipsoid. The same equations (46) hold for their images, $\tilde{\vec{Q}}_1^*$, $\tilde{\vec{Q}}_2^*$, $\tilde{\vec{Q}}_3^*$, $\tilde{\vec{Q}}_4^*$, after rescaling (eq 44). After the rescaling, these vectors describe spheres which are, respectively, h_1 and h_2 times larger than the critical sphere. We conclude that the rescaling of space, which maps the critical ellipsoid onto the critical sphere, does not change h_1 and h_2. One immediately gets

$$\Gamma_4(f,\{\tilde{\vec{Q}}_1^*\},\tilde{\vec{Q}}_1^*+\tilde{\vec{Q}}_2^*,\tilde{\vec{Q}}_3^*,+\tilde{\vec{Q}}_4^*,E) = \Gamma_4(f,\{\tilde{\vec{Q}}_1^*\},h_1,h_2,E) = \Gamma_4(f,x^*,h_1,h_2) \qquad (47)$$

where $\Gamma_4(f,x^*,h_1,h_2)$ denotes the fourth-order function in a zero electric field. Formulas 45 and 47 show that, if a structure, $\{\tilde{Q}^*\}$, in an electric field comes from the zero field structure, $\{\tilde{Q}^*\}$, by mapping (eq 44), their ψ-dependent parts of the free energy are equal. It allows direct application of the phase diagram calculated by Leibler[4] to describe the phase behavior of copolymer melts of class $\mathcal{A}$.

Without an electric field, the only structures proven[4] to be stable are one-dimensional lamellar (smectic A), two-dimensional triangular honeycomb, and three-dimensional body-cubic-centered mesophases. Rescaling (eq 44) maps these mesophase into lamellar (smectic C), two-dimensional monoclinic, and three-dimensional triclinic, Γ_t lattices, respectively (see Figure 14). These three low-symmetry structures appear as a birefringence of the Bravais lattices corresponding to a zero field. Two-dimensional monoclinic structures look like a rodlike mesophase with A (B)-unit-rich cylinders, which form a tessellation of congruent parallelograms filling a plane without overlapping. In the reciprocal space, the corresponding parallelograms are always inscribed in a section of the critical ellipsoid. Given f and E, the form and the size of the parallelogram depend upon the angle between an applied electric field and the spontaneously chosen direction of these rod axis. If these rods are oriented strictly perpendicularly to the electric field, the mesophase has the symmetry of a honeycomb lattice.

Analogously, all three-dimensional monoclinic Bravais cells inscribed in the critical ellipsoid have the same energy. If one of the critical wave vectors is oriented along an applied field, the corresponding mesophase has the symmetry of the body-centered tetragonal lattice, Γ_0^f, shown in Figure 14.

For symmetric copolymers ($f = 0.5$), the Landau-type analysis predicts a second-order transition from the disordered phase to the lamellar patterns at the spinodal point. The phase diagram for the microphase separation of diblock copolymers of class $\mathcal{A}$ is given by Figure 5. The transition temperatures do not depend at all upon an applied electric field and are the same, respectively, as those[4] of the transition from a homogeneous melt to a body-cubic-centered phase, from the cubic-body-centered phase to a hexagonal and from the hexagonal to a lamellar phase in the absence of an electric field.

On the contrary, the periodicity of the ordered structures will depend upon the direction of the symmetry breaking with respect to an electric field. The minimum and maximum of it correspond respectively to lamellae oriented perpendicularly to or along the electric field (Figure 7).

Class $\mathcal{B}$. Two Critical Rings. When the anisotropic parts of links' polarizability tensors are different, the critical wave vectors form two rings in $\tilde{Q}$-space perpendicularly to the applied field. The critical star is seen to consist of wave vectors of the same length.

Only two ordered structures are possible for class $\mathcal{B}$: a one-dimensional (lamellar) phase and a two-dimensional phase, which has a symmetry of a planar rhombic lattice. As shown in ref 4, for the case of equal critical wave vectors (class $\mathcal{B}$ corresponds to it), the free energy of lamellar phases is always less than the free energy of rhombic structures. Thus, for class $\mathcal{B}$ the only transition from the disordered melt to the lamellar phase occurs. The phase diagram in coordinates χN and f is shown in Figure 8.

In the lamellar phase the monomer A density is a constant in a plane which makes an angle (eq 40) with the applied electric field. This angle depends upon neither the degree of polymerization, N, nor the Flory–Huggins parameter, χ, but solely on the intensity of the electric field, E, and the composition, f. The free energy of these structures is given by eqs 25 and 34 with

$$\tilde{f} = f^* \qquad \tilde{x} = \tilde{x}^*$$

For every composition f, this transition coincides with the absolute stability line:

$$(\chi N)_l(f) = (\chi N)_c(f)$$

The plots f^* and $\tilde{x}^*$ vs f are shown in Figures 9 and 10 and discussed in section 7. The spinodal line depends only upon the composition f but differs from the spinodal line in the absence of electric field if only $f \neq 0.5$. A paradox of the zero electric field limit is that for a zero electric field the composition region of class B is restricted only by $f = 0.5$. The transition line, which in the considered case coincides with the spinodal line, does not depend upon the electric field. Let us note that for any composition the transition to the lamellar mesophase from the homogeneous melt occurs as a second-order transition. The angle (eq 40) between the field and the normal to lamellar layers depends on the electric field and the composition, f.

Class $\mathcal{C}$. Two Critical Points. The only structure which appears after ordering is a lamellar structure oriented strictly perpendicularly to the electric field. The second-order transition from the disordered to this lamellar phase occurs at the spinodal line. The free energies of the lamellar phase is given by formulas 25 and 34 with

$$\tilde{f} = f_*^*(E) \qquad \tilde{x} = x_*^*(E)$$

where f_*^* is the effective composition (24) associated with the Kuhn length measured along the electric field. For several compositions the spinodal lines for copolymers of class $\mathcal{C}$ are shown in Figure 12. The value of $(\chi N)_l$ as well as the distance between the layers depend upon E. For any composition, f, the microphase separation transition occurs as a second-order one, i.e., coincides with the absolute stability limit of homogeneous melt.

Class $\mathcal{D}$. One Critical Ring. This third type of copolymer melts corresponds to the case when critical surface in Q-space is a ring (42) located perpendicularly to an applied field. The only possible mesophases are triangular honeycomb and lamellar structures. Such symmetries, for instance, would have a rode-like mesophase with $A(B)$ - units-rich cylinders along the electric field which form a tessellation of equilateral triangles, and a simple lamellar phase with layers oriented along the electric field. The periodicity (42) of the patterns depends upon the electric field.

The free energies of these structures are given by formulas 25 and 34 with

$$\tilde{f} = f_*^{**}(E) \qquad \tilde{x} = x_*^{**}(E)$$

where f_*^{**} is the effective composition (eq 24) associated with the Kuhn lengths measured perpendicularly to the electric field.

Since the body-centered-cubic phase is suppressed, the transitions from the disordered melt to the two-dimensional honeycomb lattice, $(\chi N)_{tr}$, and from the

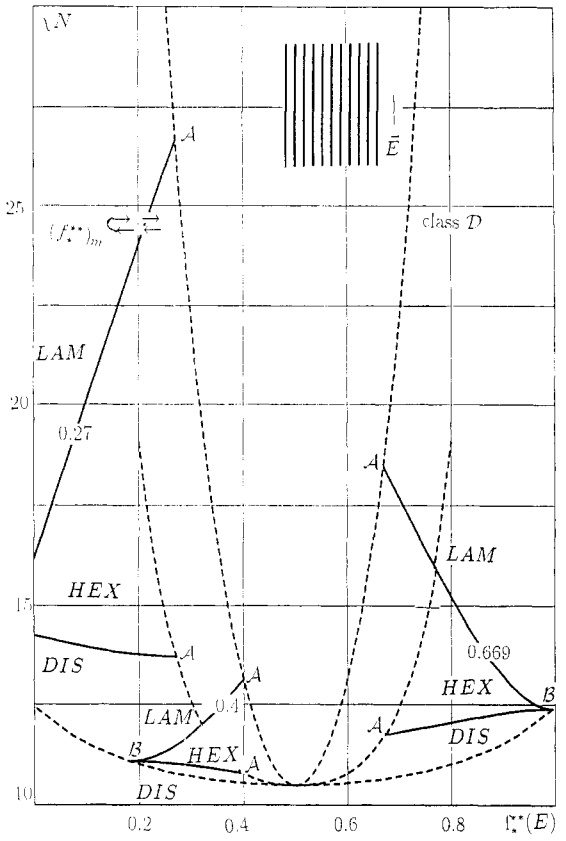

Figure 15. The phase diagram for a diblock copolymer melt of class $\mathcal{D}$ for $f = 0.4, f = 0.669$ and 0.27. It presents the region of the stability of a disordered, a honeycomb (hexagonal), and a lamellar phases in the plane with coordinates $f_*^{**}(E)$ and χN. Three dashed lines show (from bottom to top) the equilibria line of the disordered–lamellar phase for class $\mathcal{B}$ in coordinates $f_*^{**}(E) = \tilde{f}^*(f)$ and χN, the equilibria lines of a disordered–triangular and triangular–lamellar lattices for zero electric field in coordinates $f_*^{**}(E) = f$ and χN. The lamellar and triangular lattices are oriented strictly parallel to the applied electric field. The disorder–lamellar and lamellar–triangular phase transitions occur as weak first-order transitions. Arrows show a reentrant phase behavior for $f = 0.27$: triangular–lamellar–triangular with increasing electric field intensity (section 10).

latter to the lamellar phase, $(\chi N)_l$, occur, respectively, for

$$(\chi N)_{tr}(f,E) = (\chi N)_c - \frac{\alpha_{tr}^2}{\beta_{tr}}$$

$$(\chi N)_l(f,E) = (\chi N)_c + \frac{9(\gamma_{tr}^2 - 1)\alpha_{tr}^2}{64\beta_{tr}}$$

where functions γ_{tr}, α_{tr}, β_{tr} in terms of vertices (eq 34) were defined in ref 4. $(\chi N)_l$ and $(\chi N)_{tr}$ transition lines depend upon the intensity of the applied field, E. For class $\mathcal{D}$, the weak first-order transition occurs directly from the disordered to the triangular lattice, the three-dimensional structures being suppressed by an electric field. For several different compositions, the phase diagrams in coordinates χN and f_*^{**} are given in Figure 15.

10. Induced Reentrant Microphase Separations

We will show below that, for the case of simultaneously positive (or negative) anisotropic polarizabilities of the A and B units, the electric field induces reentrant microphase separation (order → disorder → order) or reentrant melting (disorder → order → disorder).

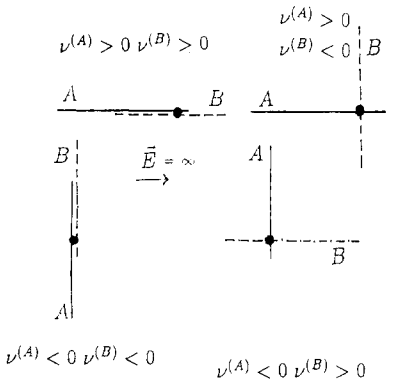

Figure 16. The A and B block copolymer conformations (schematic) in the limit of infinite electric field.

Class $\mathcal{C}$: $\nu^{(A)} > \nu^{(B)} > 0$ or $\nu^{(A)} < \nu^{(B)} < 0$. If the anisotropic polarizabilities of A and B units, $\nu^{(A)}$ and $\nu^{(B)}$, are both positive (or negative), in the limit of infinite electric field, the conformations of both blocks are described by one-dimensional random walks along (perpendicular) the applied field (see Figure 16). The effective composition associated with the statistical segments of blocks measured along the infinite field, f_*^*, is equal to that in zero electric field:

$$\frac{f_*^*}{1 - f_*^*} = \frac{(R_1^{(A)})^2}{(R_1^{(B)})^2} = \frac{N_A}{N_B} = \frac{f}{1 - f}$$

Though the same for zero and infinite electric fields, the effective composition, f_*^*, differs, in general, from the composition f for intermediate values of the electric field intensity. Thus, the effective composition reveals a reentrant behavior: with increasing field, f_*^* takes on its values twice. Since for class $\mathcal{C}$ the phase behavior depends only on f_*^*, this reentrant behavior of f_*^* should promote *reentrant microphase separations and melting*.

Let us consider first the case when A units are oriented along $\vec{E}$ more readily than B units ($\nu^{(A)} > \nu^{(B)} > 0$ or $\nu^{(B)} < \nu^{(A)} < 0$). In such a case the effective composition, f_*^*, is larger than f. Being the same for the limits of zero and infinite fields, the composition f_*^* has a maximum, $(f_*^*)_m$, as is depicted in Figure 12. As shown, there is reentrant microphase separation: lamellar structure → disordered melt → lamellar structure with increase of E.

A similar analysis can be developed for the other cases.

Class $\mathcal{C}$: $\nu^{(B)} > \nu^{(A)} > 0$ or $\nu^{(B)} < \nu^{(A)} < 0$. In this case, a melt of class C should reveal disordered phase → lamellar structure → disordered phase reentrant melting with increasing E.

Class $\mathcal{D}$ for $\nu^{(A)} > \nu^{(B)} > 0$ or $\nu^{(A)} < \nu^{(B)} < 0$. Lamellar → molten → lamellar or hexagonal → molten → hexagonal phase reentrant separations are revealed.

Class $\mathcal{D}$ for $\nu^{(B)} > \nu^{(A)} > 0$ or $\nu^{(B)} < \nu^{(A)} < 0$. The increase of E leads to disordered → lamellar → disordered phase and disordered → hexagonal → disordered phase reentrant melting.

11. Discussion

We have studied possible phase transitions in an amorphous diblock copolymer melt in an electric field. The essential conclusion is that, at equilibrium, the properties of a melt are determined according to which of the four universal classes it belongs. The class is determined by only three relevant parameters: the copolymer chain composition, f, and the parameters $S^{(A)}$

and $S^{(B)}$, which characterize the birefringence of A and B blocks, that is, how many times the square of the radii of gyration of blocks along an electric field are larger (smaller) than those in a zero electric field. The results are summarized in a universal diagram (Figure 13), which presents the composition regions of different classes.

Each of these classes reveals its specific X-ray scattering patterns for the disordered state near the spinodal point, its specific dependence of transition temperatures on an electric field, and its specific cascade of phase transitions while microphase separating. Four universal phase diagrams (Figures 5, 8, 12, and 15) present the regions of stability of different phase for different classes.

How does one define, experimentally, the composition regions of the universal classes? We suppose two independent experimental methods of measurement of parameters $S^{(A)}$ and $S^{(B)}$. First, given an applied electric field, these parameters can be calculated by definition 8, the anisotropic part of the unit polarizability, ν, being known. The fact that the nonlinear part of the dielectric polarizability of a homopolymer melt is sensitive to the anisotropic part of the unit polarizability provides a direct method of measuring of the latter. For instance, by measuring the nonlinear part of the dipole moment per unit volume for a thin slap of homopolymer melt oriented along the field (see equations 14), the anisotropic polarizabilities of the units should be extracted directly. For the experimental geometry of the work,[3] the anisotropic part of the polarizability can be extracted from a simultaneous analysis of the linear and nonlinear parts of the homopolymer melt polarizability (ref 17) (Appendix C). Finally, polarization data for statistical segments may be found in the literature.[15,18]

Another astuce is to extract the parameters $S^{(A)}$ and $S^{(B)}$ from equation 11, which relates the radius of gyration of a homopolymer chain along the electric field to that perpendicular to it:

$$\frac{R_l^2}{R_p^2} = \frac{2S}{3-S}$$

or from relation of the radius along the field to that in zero electric field:

$$\frac{R^2}{R_l^2} = \frac{1}{S}$$

[But the reader has to keep in the mind that for the same applied external electric field, $\mathcal{E}$, and for the same geometry of experiments, the internal electric field, E, which gives rise to chain birefringence, in homopolymer and copolymer melts differ from each other (sections 3 and 4).] For a given experimental geometry and given electric field, parameters $S^{(A)}$ and $S^{(B)}$ being extracted, the class of copolymer melt follows directly from the tabulated curve shown in Figure 13. Symmetric diblock copolymers is seen to belong to class $\mathcal{B}$.

An increase of the electric field leads to transitions between different classes (section 7). For instance, lamellar phase oriented perpendicularly to the electric field (class $\mathcal{O}$) should be spontaneously transformed (by an orientational phase transition) in lamellar phase oriented parallel to the field (class $\mathcal{B}$). These orientational reformations of the patterns are real *second-order* phase transitions equivalent to the *smectic A* → *smectic C* → *smectic A* transitions in liquid crystals.

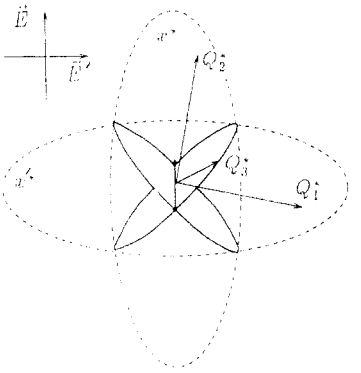

Figure 17. A transformation of a pattern with a tilting of the applied electric field ($\vec{E} \rightarrow \vec{E}'$) for a copolymer melt of class $\mathcal{A}$.

What are the typical peculiarities of renumerated classes? Class $\mathcal{A}$ represents strongly degenerated-in-electric-field copolymers, for which the anisotropic parts polarizabilities of the A and B segments are equal. When χN is smaller than $(\chi N)_m$, a melt exhibits the disordered phase. Radiation-scattering experiments provide a good method of studying this phase. Near the spinodal point monomer density fluctuations should reveal a very specific spectrum with a maximum scattering at vectors which form a symmetrical ellipsoid with the principal axis oriented along the electric field. Following the order–disorder transition, mesophases with nonfixed periodicities must appear. The periodicity ranges between some maximum and minimum values and depend upon the direction of the symmetry breaking with respect to the electric field. Given the copolymer composition and an electric field, the patterns will not be reproducible, from one experiment to another. For instance, lamellae oriented differently with respect to the applied field will have different periodicities.

While increasing χN, a cascade of weak, first-order transitions occurs: three-dimensional triclinic → two-dimensional monoclinic → one-dimensional lamellar structure. If a pattern appears spontaneously oriented along the electric field, the first two structures are body-centered-tetragonal and triangular structures. These results are summarized in Figure 5, which presents regions of the stability of different phases in the plane with coordinated χN and f. The spinodal line for class A is shown in Figure 4.

While changing the intensity of the electric field, class A remains isomorphic to itself: neither the spinodal line nor the first-order transition lines will be shifted. Evidently they are equal to those of Leibler for zero electric field. On the contrary, the periodicity of the structures will be very sensitive to the intensity of the applied field. As an example, we consider a copolymer melt of class A with a negative anisotropic polarizability, ν, of segments. Upon diminishing the electric field intensity from E to E', the critical ellipsoid will be stretched along the electric field. The pattern periodicity along the field increases, the periodicity perpendicular to the field decreases, and for certain orientations, it does not change its value. Equation 38 gives a quantitative description of the pattern periodicity in the field.

If the electric field is tilted (change direction, $\vec{E} \rightarrow \vec{E}'$) the pattern, in general, will be transformed if only wave vectors $\vec{Q}^*$ are not located on the "butterfly" of two-ellipsoid intersection, x^* and $x^{*\prime}$ (Figure 17). In the latter case, no pattern modification occurs while the electric field is tilting.

For class $\mathscr{B}$, critical fluctuations are concentrated in Q-space in two rings perpendicular to the electric field. X-ray scattering experiments should show this.

For a given composition, f, and an applied field, E, the angle between the field and the direction along which the microphase separation pattern appears is fixed. This angle (equation 40) reveals a complicated dependence on the electric field intensity but is determined only by f, $S^{(A)}$, and $S^{(B)}$.

When χN is smaller than the value $(\chi N)_c$, calculated with the aid of eq 39, a melt exhibits a disordered phase. At $(\chi N)_c$, a second-order transition occurs from disordered to lamellar phase without any intermediate structures for any composition, f. The essential result is that the transition temperature does not depend at all on the electric field. However it is different from that of Leibler for zero electric field for $f \neq 0.5$. An apparent contradiction for zero electric field limit is that the composition region of a class $\mathscr{B}$ copolymer in zero electric field collapses to composition $f = 0.5$, for symmetric copolymers. On the contrary, for very strong electric fields, class $\mathscr{B}$ should cover a large region of the compositions (Figure 13). Upon tilting the electric field, the lamellae of class $\mathscr{B}$ will be aligned.

For class $\mathscr{C}$, only fluctuations with wave vectors (eq 41) oriented strictly along an electric field diverge at the spinodal point. The transition temperature from the disordered to the lamellar phase will always be shifted to smaller $(\chi N)_l$ values than that calculated for zero electric field (for class $\mathscr{A}$), but it will always be larger than that calculated for class $\mathscr{B}$). For any composition f, the lamellar phase oriented perpendicularly to the electric field appears by a second-order transition from a homogeneous melt. The transition temperature and pattern periodicity do depend on the intensity of the electric field. The normal to lamellar layers will always follow the direction of the electric field.

For class $\mathscr{D}$, critical wave vectors form in Q-space the ring (eq 42) perpendicular to the electric field. For any composition, f, while increasing χN, two-dimensional honeycomb and lamellar phases oriented strictly parallel to the electric field appear by first-order transitions. The transition temperatures and the pattern periodicity depend on the electric field.

The spinodal line is given in Figure 12. The phase diagram is shown in Figure 15. The transition temperatures from the disordered to the lamellar and from the lamellar to the hexagonal structures will always be shifted to other $(\chi N)_l$ values than those calculated for zero electric field (Figure 18). Upon tilting the electric field, lamellar and triangular structures will be tilted. The only exception is a lamellar phase oriented strictly perpendicularly to the plane of the electric field tilting.

The theory also predicts field-driven *reentrant microphase separations or reentrant microphase melting*. For the case of simultaneously positive or negative anisotropic polarizabilities of the A and the B units, a ordered → disordered → ordered or disordered → an ordered → disordered reentrant transitions should be induced by increasing electric field in diblocks of classes $\mathscr{C}$ and $\mathscr{D}$ (section 9).

All these effects should be observable to provide a detailed verification of the theory. Unfortunately, until now, systematic experimental studies of copolymers under strong electric fields were not available. We hope that the suggested picture of microphase separation will be helpful for detailed treatments of experimental results on liquid crystalline and sheared copolymers. As to electric field, the most interesting phenomena, such as reentrant separations and orientational transitions,

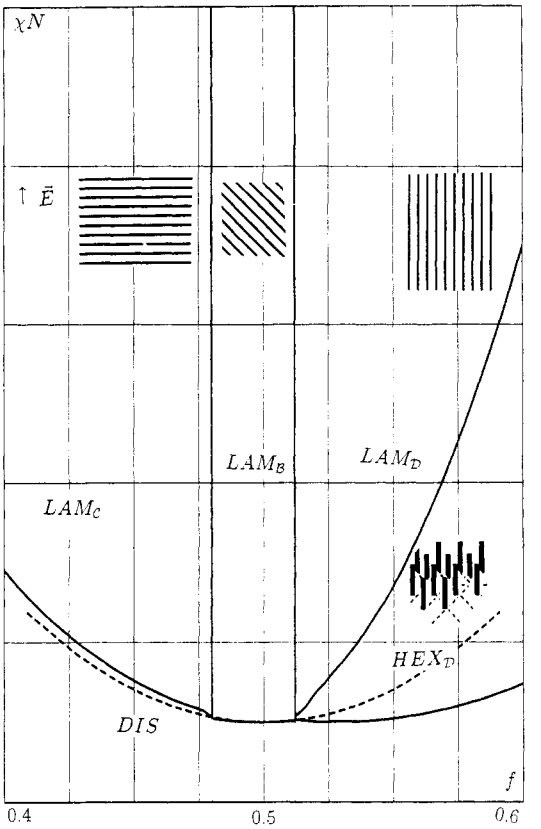

Figure 18. A typical phase diagram of a block copolymer melt in an electric field of 10^8 J C^{-1} m^{-1} at 25 °C; $\nu^{(A)}$ and $\nu^{(B)}$ are both 10^{-38} C^2 m^2 J^{-1}. The dashed line is the spinodal for zero electric field.

will be observable, unfortunately, only for very symmetric diblocks. Indeed, let us consider a block copolymer melt with the anisotropic parts of the electronic polarizabilities of A and B statistical units, $\nu^{(A)}$ and $\nu^{(B)}$, equal to 10^{-38} C^2 m^2 J^{-1} and -10^{-38} C^2 m^2 J^{-1}. Here and in what follows we use the SI system. (In units 10^{-40} C^2 m^2 J^{-1} the electronic polarizabilities of molecules CH_2CH_2, C_6H_6, and $CHCl_3$ are[18,15] 4.3, 8.2, and 10.3, respectively, but A and B statistical segments can include about $10-10^2$ such chemical monomers). In an electric field of 10^8 J C^{-1} m^{-1}, which is at the limit of the dielectric strength of polymeric liquids, at 25 °C (i.e., for $kT = 4 \times 10^{-21}$ J), the parameters $S^{(A)}$ and $S^{(B)}$ are 1.09 and 0.91; Figure 13 shows that even in this case, class B covers an extremely narrow region of the compositions: from 0.485 to 0.512. The phase diagram of the melt is shown in Figure 18.

The described picture suggests numerous applications of electric field-induced phenomena. Indeed, the electric field plays the same role as the χN parameter or the composition f. The electric alignment of lamellar structures could be used to tailor anisotropical properties of copolymer materials and to create monodomain structures. The electric field shifts the temperatures of the order–disorder transition and transitions between different mesophases. In particular, it suppresses a body-centered-cubic phase in the phase diagram. Thus, it can be applied as a very active and multipurpose parameter in block copolymers.

It is important to point out limitations of the theory. Firstly, the dipole–dipole interaction has been taken into account self-consistently. Secondly, the picture of four universal classes was developed for the random phase approximation. Both of them are approximations of the mean-field theory. Hence, only a Landau-type analysis has been used to describe the phase transitions

between the mesophases, that is, at each step we neglected all the fluctuation effects.

The fluctuations, however, could play an important role. Leibler mentioned[4] that for the zero electric field case Brazovskii fluctuations[16] would restore the first-order character of transition from a disordered melt to a lamellar phase even for symmetric copolymers and shift the transition line. The consideration of the fluctuations in the case of an electric field requires a rather refined and complicated analysis. Indeed, the composition fluctuations result in the fluctuation of the internal electric field due to the composition-pattern-dependent dielectricity of the melt. The chain conformation at the given point will depend upon the internal electric field, which, in turn, is a function of the local order parameter value. Our project is to introduce fluctuational effects. However, the picture of four universal classes hardly requires essential revisions by fluctuations for sufficiently large electric fields.[19]

Finally, we did not address weak corrections to the dipole–dipole electrostatic energy coming from the space modulation of the composition.[3,14] First, these corrections are not related to the polymeric nature of the problem; i.e., they would exist even in a mixture of monomeric dipoles. Second, the Flory–Huggins energy itself comes from a space modulated part of the dipole–dipole interaction between spontaneously induced dipoles (van der Waals forces). Since these dipoles, spontaneously induced by the fluctuating microscopic molecular electric,[8] are much stronger than permanent dipoles induced by an applied field, this correction to the electrostatic energy is small in comparison with the Flory–Huggins term. In experiments the electrostatic correction can lead to a small shift of χ.

Acknowledgment. This work was supported by the Elf-Aquitaine Co. and CNRS contracts and performed during my stay at Laboratoire de Physico-Chimie Theorique, ESPCI, in Paris. Studying and working on polymer physics I had a chance to collaborate with Jacques Prost and Ludwik Leibler and benefited from numerous discussions with them. The essential points of the present work as well as the choice of the problem itself were inspired by these conversations.

I would like to hope that in this work the spirits of two scientific schools, Landau Institute for Theoretical Physics and Laboratoire de Physico-Chimie Theorique, ESPCI, are reflected and lead to an experimentally verifiable picture, arising from and supported by properly chosen methods of theoretical physics.

I am also grateful to A. Balazs, J.-P. Carton, I. Eruchimovich, and J.-F. Joanny for their interest in and attention paid to the work.

Appendix A. Conformation of an Ideal Chain in an Electric Field. In this appendix we calculate the end-to-end distribution function of a freely jointed, noninteracting chain in an electric field through microscopic polarizability tensor of units.

The probability that the chain with the Ith unit at point $\vec{r}_I$ has the Jth unit at point $\vec{r}_J = \vec{r} + \vec{r}_I$, $P_{IJ}(\vec{r})$, is

$$\int \delta(\vec{r} - \sum_{K=I}^{J} \vec{a}_K) P(\{\vec{a}_K\}) \prod_{K=I}^{J} d\vec{a}_K,$$

where $P(\{\vec{a}_K\})$ is the conformational distribution function. Using the Fourier presentation of the δ-function, the previous expression is rewritten as

$$P_{IJ}(\vec{Q}) = \prod_{K=I}^{J} \int p(\vec{a}_K) e^{-i\vec{Q}\vec{a}_K} \, d\vec{a}_K \tag{48}$$

where $p(\vec{a}_K)$ is the link distribution function. In an electric field the probability that the Kth link be oriented as $\vec{a}_K$ is

$$\begin{aligned} p(\vec{a}_K) &= \frac{\exp\{\vec{E}\vec{P}_K/(kT)\}}{\int \exp\{\vec{E}\vec{P}_K/(kT)\} \, d\vec{a}_K} \\ &= \frac{\exp\{E_i \alpha_{ij}(\vec{a}_K) E_j/(a^2 kT)\}}{\int \exp\{E_i \alpha_{ij} E_j/(a^2 kT)\} \, d\vec{a}_K} \\ &= \frac{\exp\{\nu(\vec{a}_K \vec{E})^2/(a^2 kT)\}}{\int \exp\{\nu(\vec{a}_K \vec{E})^2/(a^2 kT)\} \, d\vec{a}_K} \end{aligned} \tag{49}$$

We have substituted expressions 3 and 4 for the dipole moment of the Kth unit and discarded the factor

$$\exp\left(-\frac{(\alpha + \nu/3)E^2}{kT}\right)$$

Since we are interested in the small $\vec{Q}$ region (in chain behavior over macroscopic scales), we consider $\vec{Q}$ vectors such that $Qa \ll 1$. In such a case the expansion $\exp(-i\vec{Q}\vec{a}_K)$ with respect to $\vec{Q}\vec{a}$ in integrals 49 is justified.

$$\int d\vec{a}\, p(\vec{a}) e^{-i\vec{Q}\vec{a}} \simeq \int d\vec{a}\, p(\vec{a}) \left\{1 - i\vec{Q}\vec{a} + \frac{(\vec{Q}\vec{a})^2}{2}\right\} \tag{50}$$

This Taylor expansion over qa is a classical trick for the calculation of the end-to-end distribution function,[6] when $\sin(qa)/(qa)$ is approximated as $1 - (qa)^2/6$. The first integral on the right hand of eq 50 identically equals one, the distribution function $p(\vec{a})$ being normalized. The second adding is evidently zero. The third integral over $\vec{a}$ can be evaluated through an appropriate choice of polar coordinates: r, θ (ranging between 0 and π), and ϕ (ranged between 0 and 2π), and we define the reference axis of θ being taken along the electric field vector, $\vec{E}$. In the polar coordinates, the distribution function of segments is

$$p(\vec{a}_K) = \frac{\delta(|a_K| - a)}{2\pi a^2} \frac{e^{\xi \cos^2\theta}}{\int e^{\xi \cos^2\theta} \sin\theta \, d\theta}$$

and

$$\int d\vec{a}\, p(\vec{a}) \frac{(\vec{Q}\vec{a})^2}{2} = \frac{\int\int e^{\xi \cos^2\theta} \sin\theta}{2\int e^{\xi \cos^2\theta} \sin\theta \, d\theta} (aQ_l \cos\theta + aQ_p \sin\theta \cos\phi)^2 \, d\theta \, d\phi = (a^2/6)\{Q_l^2 S + Q_p^2(3 - S)/2\} \tag{51}$$

where Q_l and Q_p are components of the wave vector directed respectively along and perpendicularly to an applied field, $\vec{E}$. Substituting eq 51 into eq 48, we obtain with the same accuracy Fourier transform of the end-to-end distribution function for a chain in an electric field:

$$P_{IJ}(\vec{Q}) = \{\int d\vec{a}_K\, p(\vec{a}_K) e^{-i\vec{Q}\vec{a}_K}\}^{|J-I|} = \left\{1 - \frac{x}{N}\right\}^{|J-I|} \simeq \exp\left(-\frac{x|I-J|}{N}\right)$$

where

$$x = (Q_l R_l)^2 + (Q_p R_p)^2$$

We supposed above that $|J - I| \gg 1$.

Appendix B. End-to-End Distribution Function in an Electric Field. The distribution function for a homopolymer chain in an electric field is evaluated through the appropriate choice of the orthogonal coordinate axes: let Q_l be directed along the electric field and Q_{p1}, Q_{p2} be directed perpendicularly to it, $Q_{p1}^2 + Q_{p2}^2$ being Q_p^2, $Q_p^2 + Q_l^2$ being Q^2. As usual (see, for instance, ref 6, sections 2.1.1–2.1.3 or ref 15, the problem in section 111) one gets

$$P_N(\vec{r}) = \int P_N(\vec{Q}) \exp i\vec{Q}\vec{r} \frac{d^3q}{(2\pi)^3} = \int \exp\left(-\frac{Na^2}{6} Q_l^2 S\right) \exp iQ_l r_l \frac{dQ_l}{2\pi} \times \prod_{j=1}^{2} \int \exp\left(\frac{Na^2}{6} Q_{pj}^2 \frac{3-S}{2}\right) \exp iQ_{pj} r_{pj} \frac{dQ_{pj}}{2\pi} = \exp\left(-\frac{3}{2} \frac{r_l^2}{NSa^2}\right) \prod_{j=1}^{2} \exp\left(-\frac{3}{2} \frac{2r_{pj}^2}{N(3-S)a^2}\right) = \exp\left(-\frac{3}{2} \frac{r_l^2}{NSa^2} - \frac{3}{2} \frac{2r_p^2}{N(3-S)a^2}\right)$$

All the normalizing constants above were omitted.

Appendix C. Solution of the Self-Consistent Equations for an Electric Field in a Polymer Melt. The solution is presented as an expansion of the internal electric field, E (or the polarization, P), in powers of the external electric field, $\mathcal{E}$. Up to the second-order term, the parameter S is

$$S = 3\frac{\int_0^1 \zeta^2 e^{\xi\zeta^2} d\zeta}{\int_0^1 e^{\xi\zeta^2} d\zeta} \simeq 1 + \frac{4}{15}\xi$$

Up to third-order, the dipole moment (eq 13) is

$$P = \left(\alpha + \frac{\nu}{3}\right) NE + \frac{4\nu^2}{45kT} NE^3 \qquad (52)$$

By substitution of the above expression in eq 17 for the internal electric field, we get, up to the third-order term, the result

$$\mathcal{E} = E\left\{1 + \frac{4\pi}{\nu}\alpha + \frac{\nu}{3}\right\} + \frac{4}{45}\frac{4\pi}{\nu}\frac{\nu^2}{kT}E^3 \qquad (53)$$

In the linear approximation, which corresponds to a nondeformed (Gaussian) chain, the relation between external and internal electric fields is given by the first term of the right hand of eq 17.

Appendix D. Nonlinear Correlation Function of a Copolymer in an Electric Field. In this appendix we demonstrate the calculation of the correlation functions for a quasi-noninteracting copolymer chain in an electric field. The results presented here are applicable not only to chains deformed by an electric field and not only to the diblock architecture but also to other systems composed of chains with an arbitrary distribution of A and B units. As an example, we calculate here the third-order correlator, $G^{(3)}_{112}$.

Following Appendix B of ref 4, let us introduce the function $\theta_I^{(i)}$, which characterizes the distribution of units A and B in the copolymer chain: when $i = 1$ (which corresponds to A units) $\theta_I^{(1)} = 1$ when the Ith unit is of type A and $\theta_I^{(1)} = 0$ when the Ith unit is of type B. Similarly, $\theta_I^{(2)} = 1$ when the Ith unit is of type B and $\theta_I^{(2)} = 0$ when the Ith unit is of type A. With the help of these notations, we obtain

$$G^{(3)}_{112}(E,f,\vec{Q}_1,\vec{Q}_2,\vec{Q}_3) = \sum_{I=1}^{I=NJ=NK=N} \sum_{J=1} \sum_{K=1} \theta_I^{(1)}\theta_J^{(1)}\theta_K^{(2)} G^{(3)}_{IJK}(E,f,\vec{Q}_1,\vec{Q}_2,\vec{Q}_3) \qquad (54)$$

where $G^{(3)}_{IJK}$ denotes the density correlation function of segments I, J, and K defined in ref 4. For chains, conformations of which are independent, the correlator $G^{(3)}_{IJK}$ is proportional to the probability, $P_{IJK}(E,f,\vec{r}_1,\vec{r}_2,\vec{r}_3)$, that in an electric field, E, the chain with the Ith unit at the point $\vec{r}_1$ has the segments J and K at points $\vec{r}_2,\vec{r}_3$, respectively:

$$P_{IJK}(\vec{r}_1,\vec{r}_2,\vec{r}_3) = G^{(3)}_{IJK}(\vec{r}_1,\vec{r}_2,\vec{r}_3) \qquad (55)$$

Indeed, relations B.1–B.5 and B.7–B.16 in ref 4 are applicable not only to a melt of Gaussian chains but also to any noncompressible melt of chains, provided that the partition functions of the chain conformations are undependent. This is the very same case as for quasi-noninteracting chains (sections 2–4).

In spite of the dipole–dipole interactions, the probability function, P_{IJK}, of quasinoninteracting chains may be expressed in terms of only pair correlators (eqs 19 and 20). Indeed, not only chains but also all the units of quasi-noninteracting chains in an electric field are distributed quisi-undependently. In Fourier space

$$P_{IJK}(E,\vec{Q}) = P_{IJ}(E,\vec{Q}_1)P_{JK}(E,\vec{Q}_3)\delta(\vec{Q}_1 + \vec{Q}_2 + \vec{Q}_3)/N \qquad (56)$$

for

$$I < J < K \bigcup K < J < J$$

Making use of formulas (19, 55, 56) we obtain for $NG^{(3)}_{112}(E,f,\vec{Q}_1,\vec{Q}_2,\vec{Q}_3)$:

$$\sum_{(1-f)NI=1}^{K=N} \sum_{J=1}^{fN} \sum_{J=1}^{fN} P^{(3)}_{IJK}(E,f,\vec{Q}_1,\vec{Q}_2,\vec{Q}_3) = \sum_{(1-f)NJ=1}^{K=N} \sum_{I=1}^{J=I} \sum_{I=1}^{fN} P_{IJ}(E,\vec{Q}_1)P_{JK}(E,\vec{Q}_3) + \sum_{(1-f)NI=1}^{K=N} \sum_{J=1}^{I=J} \sum_{J=1}^{Nf} P_{JI}(E,\vec{Q}_1)P_{IK}(E,\vec{Q}_3) = 2\int_{fN}^{N} dK \int_0^{fN} dJ \int_0^{J} dI\, P_{KJ}(E,f,Q_3)P_{IJ}(E,f,Q_1) = 2N^3 \int_f^1 dk \int_0^f dj \int_0^j di \exp\{(k-f)x^{(B)}(Q_3)\} \times \exp\{(f-j)x^{(A)}(Q_3)\}\exp\{(i-j)x^{(A)}(Q_1)\} \qquad (57)$$

where $P^{(i)}_{JK}$ correlators are given by eqs 19 and 20. The

numbers fN and $(1-f)N$ being $\gg 1$, the replacement of the summation in eq 54 by an integration was justified.

As shown in section 7 for universal class A

$$x^{(A)}(\vec{Q}) = x^{(B)}(\vec{Q})$$

In such a case, we can define a structure factor, h, as follows

$$h = \frac{x^{(A)}(\vec{Q}_3)}{x^{(A)}(\vec{Q}_1)} = \frac{x^{(B)}(\vec{Q}_3)}{x^{(B)}(\vec{Q}_1)} = \frac{\tilde{x}(\vec{Q}_3)}{\tilde{x}(\vec{Q}_1)} \tag{58}$$

with

$$\tilde{x}(\vec{Q}) = f x^{(A)}(\vec{Q}) + (1-f)x^{(B)}(\vec{Q})$$

For the three other classes B, C, and D, only lamellar ($_l$) and hexagonal ($_{tr}$) structures are possible near the spinodal point. For these structures, the values of $\vec{Q}_3$ are

$$|\vec{Q}_3| = |\vec{Q}_2 + \vec{Q}_1| = 0 \tag{59}$$

$$|\vec{Q}_3| = |\vec{Q}_1| \tag{60}$$

For such a case we can introduce formally a factor (eq 58), h, which equals 0 and 1 for the lamellar (eq 59) and triangular (eq 60) structures, respectively. Using the definitions of the structure factor, h, integral 57 reads as follows:

$$2N^2 \int_f^1 dk \int_0^f dj \int_0^j di \exp\{h(k-f)x^{(B)}\}\exp\{h(f-j)x^{(A)}\} \times \exp\{(i-j)x^{(A)}\} = \frac{2N^2}{(x^{(A)})^2 x^{(B)}}(1 - e^{-x^{(B)}(1-f)h})\left(\frac{1}{h} - \frac{e^{-x^{(A)}f}}{(1-h)} + \frac{e^{-x^{(A)}fh}}{h^2-h}\right)$$

All other third- and forth-order correlators can be obtained analogously. The results of the calculations are summarized in eqs 31 and 33.

Appendix E. Free Energy Expansion in an Electric Field. Transformation rules (eq 33) relate the correlator functions of quasi-noninteracting copolymer chains in an electric field with those of an ideal Gaussian copolymer chain with a formal composition, $\tilde{f}$. For the inverse matrix, G^{-1}_{ij}, one finds

$$G^{-1}_{i_1 i_2}(E) = \left(\frac{\tilde{f}}{f}\right)^{l}\left(\frac{1-\tilde{f}}{1-f}\right)^{2-l} G^{-1}_{i_1 i_2}(\tilde{x},\tilde{f})$$

where l and $2-l$ are numbers of indices, i_1, i_2, having the values 1 or 2, respectively, and G^{-1} is the inverse two-order correlator of a Gaussian chain with the composition $\tilde{f}$ calculated for the periodicity parameter $\tilde{x}$.

Subsequently one observes that in expressions 26 the summation over the repeated indices takes place only when one of the indices belongs to G^{-1}_{ij} and another to $G^{(n)}_{ij...}$. The summations of each index i_l in $G^{-1}_{i_l j}$ function results in the factors

$$\frac{\tilde{f}}{f} \qquad \frac{1-\tilde{f}}{1-f}$$

for $i_l = 1$ and $i_l = 2$, respectively. The same index in a $G^{(n)}_{...i_l...}$ function results in the reciprocal factors

$$\frac{f}{\tilde{f}} \qquad \frac{1-f}{1-\tilde{f}}$$

Summations over repeated indices discard all factors

$$\left(\frac{f}{\tilde{f}}\right)^p \left(\frac{1-f}{1-\tilde{f}}\right)^m$$

in each term of the free energy. As a result one gets immediately eq 34.

Appendix F. Assymptotic Behavior of the Light-Scattering Function for a Copolymer Melt in an Electric Field. For large and for small wave vectors, two-order response functions read

$$G^{(2)}_{11}(E) \sim \frac{f^2}{\tilde{f}^2}\frac{2\tilde{f}}{\tilde{x}}$$

$$G^{(2)}_{22}(E) \sim \frac{(1-f)^2}{(1-\tilde{f})^2}\frac{2(1-\tilde{f})}{\tilde{x}}$$

$$G^{(2)}_{(12)}(E) \sim 0$$

and

$$G^{(2)}_{11}(E) \sim \tilde{f}^2\tilde{x}^2(1+\tilde{f}\tilde{x}/3)$$

$$G^{(2)}_{22}(E) \sim (1-\tilde{f})^2\tilde{x}^2(1+(1-\tilde{f})\tilde{x}/3)$$

$$G^{(2)}_{12}(E) \sim (1-\tilde{f})\tilde{f}\tilde{x}^2(1+\tilde{x}/2)$$

respectively.

References and Notes

(1) Folkes, M. J.; Keller, A.; Skalisi, F. P. *Colloid. Polym. Sci.* **1973**, *251*, 1. Hadziioannou, G.; Mathis, A.; Skoulios, A. *Colloid. Polym. Sci.* **1979**, *257*, 136.
(2) Morrison, F. A.; Bourvellec, G. L.; Winter, H. H. *J. App. Polym. Sci.* **1987**, *33*, 1585. Morrison, F. A.; Winter, H. H. *Macromolecules* **1989**, *22*, 3533. Morrison, F. A.; Winter, H. H.; Gronski, W.; Barnes, J. D. *Macromolecules* **1990**, *23*, 4200.
(3) Amundson, K.; Helfand, E.; Davis, Don D.; Patel, S. S.; Quan, X.; Smith, D. S. *Macromolecules* **1991**, *24*, 6546.
(4) Leibler, L. *Macromolecules* **1980**, *13*, 1602.
(5) de Gennes, P. G. *Scaling Concepts in Polymer Physics*; Cornell University Press: Ithaca, NY, 1979.
(6) Doi, M.; Edwards, S. F. *The Theory of Polymers Dynamics*; Clarendon Press: Oxford, 1986.
(7) Kuhn, W. *Kolloid Z* **1934**, *68*, 2, *J. Polym. Sci.* **1946**, *1*, 360.
(8) Landau, L. D.; Lifshitz, E. M. *Electrodynamique des Milieux Continus*, T.8; Editions Mir: Moscow, 1969.
(9) Landau, L. D.; Lifshitz, E. M. *Mechanique*, T.1; Editions Mir: Moscow, 1966.
(10) Landau, L. D.; Lifshitz, E. M. *Theorie du Champ*, T.2; Editions Mir: Moscow, 1966.
(11) Gurovich, E.; Leibler, L.; Prost, J., unpublished.
(12) Amit, D. J. *Field Theory, the Renormalization Group, and Critical Phenomena*; McGraw-Hill Inc.: London, Great Britain, 1978.
(13) Lifshitz, I. M. *Soviet Phys. JETP*, **1966**, *28*, 1280.
(14) Carton, J.-P.; Leibler, L., private communication.
(15) Israelachvili, J. *Intermolecular and Surface Forces*, 2nd ed.; Academic Press: New York 1991.
(16) Brazovskii, S. *Soviet Phys. JETP* **1975**, *41*, 85. Fredrickson, G.; Helfand, E. *J. Chem. Phys.* **1987**, *87*, 697.
(17) Gurovich, E. V., Kats, E. I., Lebedev, V. V. *Soviet Phys. JETP* **1988**, *94*, 167. *Soviet Phys. JETP* **1991**, *100*, 855.
(18) Lide, D. R. *Handbook of Chemistry and Physics*, CRC Press, Inc.: Boca Raton, 1993. von Hippel, A. R., *Tables of Dielectric Materials*, Massachussetts Institute Of Technology: Cambridge, 1944–1953; Vol. 1–5. Hanper, C. A. *Handbook of Plastics and Elastomers*; McGraw-Hill, New York, 1975.
(19) As was noticed by one of the referees, for strongly modulated structures, all the harmonics will be important: Kawasaki, K., Ohta, T., Kohrogui, M. *Macromolecules* **1988**, *21*, 2972. Melenkevitz, J., Muthukumar, M. *Macromolecules* **1991**, *24*, 4199. Olvera de la Cruze, M. *Phys. Rev. Lett.* **1991**, *67*, 85.